ABSTRACT

SHEN, JIALONG. Behaviors of Poly(ε-caprolactone)s (PCLs) Coalesced from Their Urea Inclusion Compounds. (Under the direction of Dr. Alan E. Tonelli).

Guest poly (ε-caprolactone) (PCL) chains, with molecular weights ranging from ~2,000 to 80,000 g/mol, were first included in and then coalesced from inclusion compounds (ICs) with a crystalline matrix formed with host urea (U). As previously observed for PCL and other polymer guests when coalesced from their ICs formed with host cyclodextrins (CDs), upon cooling from their melts, PCLs coalesced from their U-ICs, regardless of their molecular weight, also show enhanced abilities to crystallize. Also consistent with PCL that was coalesced from their CD-ICs, coalesced PCLs (c-PCLs) obtained from their U-ICs retain their enhanced abilities to crystallize even after spending long times in the melt. Because, unlike CD hosts, U does not thread over guest polymer chains in their ICs, we conclude that the enhanced ability of c-PCLs to crystallize from their melts upon removal of either host from their ICs is solely a consequence of their coalesced conformations/ structures/morphologies, which are stable to prolonged melt-annealing and are independent of the type of host used. Small amount of c-PCLs obtained from their U-ICs are observed to effectively enhance the melt-crystallization of as-received PCL. Furthermore, c-PCLs were observed to have increased hardness and modulus by nano-indentation and tensile testing. C-PCLs obtained from U-IC elongate much more than PCL coalesced from α-CD, which is very brittle.

Behaviors of Poly(ε-caprolactone)s (PCLs) Coalesced from Their Urea Inclusion Compounds

by
Jialong Shen

A thesis submitted to the Graduate Faculty of
North Carolina State University
in partial fulfillment of the
requirements for the degree of
Master of Science

Textile Engineering

Raleigh, North Carolina

2012

APPROVED BY:

_____	_____
Dr. Alan E. Tonelli Committee Chair	Dr. Richard Kotek
_____	_____
Dr. Russell E. Gorga	Dr. Julie Willoughby

DEDICATION

This work is dedicated to my loving wife, my family, and my friends for their ardent support.

BIOGRAPHY

Jialong Shen was born in Hangzhou, Zhejiang Province, China where he received first four years elementary education before he moved to Shanghai. He finished the rest of his elementary and high school education in Shanghai. Jialong completed his undergraduate program and was conferred the Degree of Bachelor of Engineering in Textile Engineering (Textile Testing and Commerce) at Donghua University (formerly China Textile University) before he started his graduate study at NCSU in 2010. With the interest in polymer science, he joined the research group of Dr. Alan E. Tonelli where he gets to learn more about the wonderful world of polymers.

ACKNOWLEDGMENTS

I would like to thank my advisor, Dr. Alan E. Tonelli, for his invaluable guidance and help in my exploration of the world of macromolecules.

I would also like to thank the rest of my graduate committee, Drs. Richard Kotek, Russell E. Gorga, and Julie Willoughby for their precious time and assistance.

I am grateful to all the group members: Alper Gurarslan, Abhay Sham Joijode, Ganesh Narayanan, Rana Gurarslan, and Hui Yang for their timely discussions and help.

I would also like to express gratitude to Mangesh Champhekar for helping me with nano-indentation, to Birgit Andersen and Judy Elson for their helpful training on various instruments, and to Dr. Hanna Gracz for recording the NMR spectra.

Finally, thank you to all my friends and classmates for your precious friendship and support.

TABLE OF CONTENTS

LIST OF TABLES

LIST OF FIGURES

Chapter 1: Introductions

1.1 Introduction to Poly(ε-caprolactone)

1.1.1 General Information of PCL

Poly(ε-caprolactone) (PCL) is a linear aliphatic, flexible, semi-crystalline polyester, which is often used in the biomedical field due to its biodegradable/bioabsorbable nature. Because of its low melting point (T_m, ca.56~65℃) and low glass transition temperature (T_g, ca. -65~-60℃), it can be easily melt processed into various forms and its amorphous portions remain rubbery at room temperature. Besides its direct uses, several copolymers of PCL have been used as diol extenders for polyurethanes, which cannot be produced by step growth polymerization of monomers due to their low reactivity and the absence of side products that can be driven off to move the reaction equilibrium towards completion.[1, 2]

1.1.2 Degradation of PCL

The biodegradable properties of PCL first came to attention in 1973[3]. It is known that the hydrolysis and bio-degradation of PCL depend on the molecular weight and the degree of crystallinity of the polymer. Both the carboxylic acid released from hydrolysis processes and many microbes and enzymes in nature catalyze the degradation of PCL.[4] The longer hydrophobic constituent of PCL, as compared to Poly(lactic acid), accounts for its longer degradation time, since hydrolytic chain scission of the ester linkage is identified as the main

abiotic degradation mechanism.[5] In addition, degradative studies showed that lipase boosts the degradation rate of PCL resulting in oligomers and monomers within 4 weeks, while there was no detectable degradation of PCL for more than two months when lipase was absent.[6]

Understanding of PCL thermal stability, on the other hand, is crucial for deciding and improving melt processing conditions. A pyrolysis degradation study showed that the degradation mechanism depends on temperature; PCL degrades by chain end scission at higher temperatures and by random chain scission at lower temperatures.[7] However, other researchers proposed different thermal degradation mechanisms, which possess their own merits.[8]

1.1.3 Synthesis of PCL

There are two general pathways for preparation of PCL; i.e., the polycondensation of hydroxycaproic acid and the ring-opening polymerization (ROP) of ε-caprolactone, which was first proposed in 1930s.[4]

Polycondensation of hydroxycaproic acid, although doable by removal of byproduct in order to drive reaction towards completion, is inherently deficient in terms of resultant polymer molecular weight and polydispersity.[9] Ring-opening polymerization of lactone, on the other hand, yields polymers with high molecular weight and low polydispersity.[10] (See Figure 1) According to different type of catalyst used, ROP can be generally divided into four types; i.e., anionic, cationic, monomer-activated and coordination-insertion.[4] Anionic ROP opens

monomer at the acyl oxygen bond and suffers from intramolecular transesterification, i.e., back-biting, which significantly lowers molecular weight of the polymer by forming cyclic oligomers and polymers. Cationic ROP is driven by bimolecular nucleophilic substitution between cationic species and the carbonyl oxygen of the monomer. In monomer-activated ROP, catalyst was used to activate the monomer and therefore attach it onto the growing polymer chain. Coordination-insertion ROP is possible by coordinating the monomer to metal catalyst followed by inserting the monomer into metal-oxygen bond in catalyst. It is reported to be the most commonly used mechanism of ROP.[4]

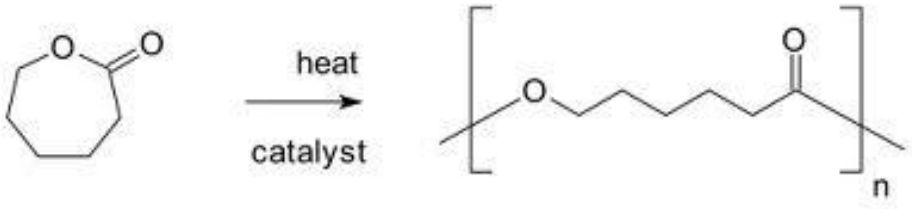

Figure 1 Chemical reaction formula of ring-opening polymerization of PCL

1.1.4 Crystallization of PCL

The study of the melt-crystallization profile of a polymer is of both scientific interest and industrial importance, and gives us an insight into the fundamental physics of polymers, as well as a better means of exploiting potential applications.

PCL is generally considered a fast crystallizing polymer in comparison to other polyesters, such as Poly-L-lactide (PLLA), which has a pendent methyl group and reduced number of

flexible methylene units, and polyethylene terephthalate (PET), which has aromatic rings along its backbone. The crystallization process of PCL has been intensively investigated as part of the study of blending PCL with other polymers,[11-13] blockcopolymers,[14, 15] inorganic particles,[16] and some other inorganic-organic hybrid materials.[17]

Although important, reports on the crystallization kinetics and morphological studies of unblended PCL are less abundant. Phillips et al.[18] realized this problem and did some experiments using unblended PCL with different molecular weights. They found to some extent that the behavior of PCL crystallization was similar to that of polyethylene (PE), as can be expected from the similar crystal structure and large portion of the same repeating units. However, the differences, between PCL and PE and among PCLs with different molecular weight, were also significant in terms of surface free energy and rate of crystal thickening.

Chen et al.[19] discussed the effects of molecular weight on the spherulite growth rate and nucleation density, where the spherulite growth rate showed a maximum at moderate molecular weights, while the nucleation density of PCL spherulites increased with increasing MW. Although not noted by these authors, the nucleation density of spherulites should gradually flatten and approach a certain maximum. The primary nucleation rate was found to be more dependent on the degree of supercooling than the growth rate was, and so were their dependence on the molecular weight.

Dhanvijay et al.[20] studied both isothermal and non-isothermal crystallization kinetics of PCL.

The former crystallization has several sets of models available, while the latter has conditions that resemble what is really happening in industrial processing. The Avrami model was found to be the best in describing isothermal crystallization, with the diagnostic parameter n in the range 2.5-3, which is indicative of three-dimensional heterogeneous nucleation with spherical crystal geometry. Non-isothermal crystallization revealed a more complicated mode of spherulitic nucleation and growth during primary crystallization and a lower dimensional space extension during secondary spherulite crystallization.

Christoph Schick and Bernhard Wunderlich are interested in semi-crystalline polymers and calorimetry. In their collaborative work[21] , PCL was chosen to be the model fast crystallizing polymer on a time scale covering from 10^{-4}s to 10^{5}s and in a temperature ranging from 25K below the glass transition to the equilibrium melting point. Traditional DSC normally has a heating or cooling rate lower than 50Kmin^{-1} but in extreme cases goes to the limit of a cooling rate up to 500Kmin^{-1}. However, it still does not meet the experimental requirement of a cooling rate more than 7000K/s in order to avoid both crystallization and nucleation during cooling. By reducing the mass of sample used, differential fast scanning calorimetry (DFSC) is able to characterize small mass sample (ca. 20ng) with a heating or cooling rate of thousands of degrees per second. It was found that at a cooling rate faster than 500K/s, crystallization was eliminated on cooling and therefore the melting endotherm equals to the cold crystallization exotherm on heating. Even faster cooling resulted in the reduction of nucleation and the subsequent cold crystallization enthalpy, which approaches a constant at cooling rates more than 5000K/s. This saturation effect was believed to be the result of

heterogeneous nuclei from unavoidable impurities.

Stefano Acierno et al.[22] utilized rheological techniques to study PCL crystallization kinetics and found that viscoelastic properties increased only at relatively high degrees of crystallinity, and that it is independent of temperature. The crystallization process was seen as a gelation process and it showed an Arrhenius type behavior. To sum up, although some new ideas have emerged and brought challenges to some previously developed theories, such as Hoffman-Lauritzen theory, general understanding of polymer crystallization still has not been met.[21]

1.1.5 Applications of PCL

PCL is degradable by both hydrolysis and organisms, and is gaining more and more interest for applications ranging from agricultural to biomedical uses. It is a soil-degradable material that has been used as seedling containers as well as shopping bags.[23] Because of its low Tg, high permeability at body temperature, and slow degradation rate, PCL has been widely recognized in controlled drug release applications.[24] Various formulations such as microspheres, nanoparticles, micelles, films scaffolds, nano-fibers, etc. are feasible. Dash[6] et al. reviewed a wide range of formulations for specific drugs and their respective preparation methods. Sinha[25] et al. wrote a comprehensive review on PCL microspheres and nanospheres, their preparation, and their specific uses. The tailorable properties of PCL achieved by copolymerization or blending with many other polymers facilitate its application for different purposes.[6]

1.1.6 Modification of PCL—Copolymerization and Blending

Because of the lower hydrolysis rate of PCL compared to other aliphatic polyesters, there were some approaches proposed to increase its degradation rate. The most used one is copolymerizing ε-caprolactone with some other lactones; e.g., glycolide and lactide. A wide range of properties were achieved through copolymerization depending on the composition.[24]

Eastmond[17] reviewed PCL blended with fair amounts of other materials, both polymeric and inorganic. Polymers of high glass transition temperature are often blended with low glass-transition temperature substances to confer flexibility and toughness to it. Conventional small molecule plasticizers have a tendency of leaching out of polymer matrices after a long period of time and therefore polymeric plasticizers were introduced.[17] However, most polymer pairs are inherently immiscible. The free energy of mixing $\Delta G_{mix} = \Delta H_{mix} - T\Delta S_{mix}$, and for spontaneously miscible polymer pairs, their thermodynamic free energy of mixing $\Delta G_{mix} < 0$. Because of their long chain nature, ΔS_{mix} is very small. The sign of ΔG_{mix} largely depends on the sign and extent of ΔH_{mix}. Furthermore, most polymer pairs exhibit endothermic mixing that is $\Delta H_{mix}>0$, leading to $\Delta G_{mix} > 0$. Therefore, most polymer pairs are inherently immiscible under standard conditions. [26] PCL is one of a small number of polymers that have been reported miscible with many other polymers, and is of interest to function as a polymeric plasticizer.[17]

Despite the versatility and applicability, there is no intention to summarize and catalogue all possible applications and modification of PCL in the current work, because PCL blends and copolymers have already been intensively investigated. The interest of this work lies in

physically modifying pure PCL to achieve elevated mechanical properties without addition of any heterogeneous immiscible component.

1.2 Inclusion Phenomena

1.2.1 The Idea of Nano-structuring

Despite the unique and valuable properties discussed above, PCL is not a strong material in terms of mechanical properties which is crucial for load bearing biomedical applications. However, if it is possible to maintain its unique properties and strengthen its physical properties in a way absent of changing its chemistry, PCL will no doubt be the most promising material in the biomedical industry. In light of this, there came the idea of nano-structuring PCL by reorganizing individual chains to a more extended less entangled conformations and configurations.

Papers from Tonelli's group pointed to the fact that polymer chains are isolated and adopt more extended conformations in their narrow inclusion compound channels.[27-39] If the extended conformations can be retained to some extent after removal of the host molecules, the resultant materials should have distinctive structures, morphologies, and conformations compared to bulk samples made from their randomly coiling melts and solutions.[40-50]

1.2.2 Introduction to Inclusion Compounds (ICs)

There are a large number of molecules that are capable of forming inclusion compounds, which can be defined as a complex where one species (the guest) is confined or trapped in another species (the host). There are two types of host molecules that are able to form inclusion compounds containing long channels. The first type is of course those molecules possessing cavities themselves, which are large enough for the threading of guest molecules. Cyclodextrins and other cyclic molecules such as crown ethers and cryptands lie in this category.[51] The second type of molecules does not have cavities themselves but their crystallographically well defined crystalline IC matrices do.[52] Upon removal of guest molecules, the host crystalline structure will undergo deconstruction. A wide range of inorganic materials such as Werner Compounds, Hofmann-Type Compounds, and aluminosilicates were reported to form inclusion complexes.[51] Organic small molecular weight species that form inclusion compounds include: urea, thiourea, perhydrotriphenylene (PHTP)[27, 29, 53], hydroquinone (HYD), etc. Figure 2 shows both type 1 (bottom two with cavities) and type 2 (top five small molecules) host species that form inclusion compounds with some other guest species. Figure 3 gives schematic view of host and guest spacing for both type 1 and type 2 host molecules.

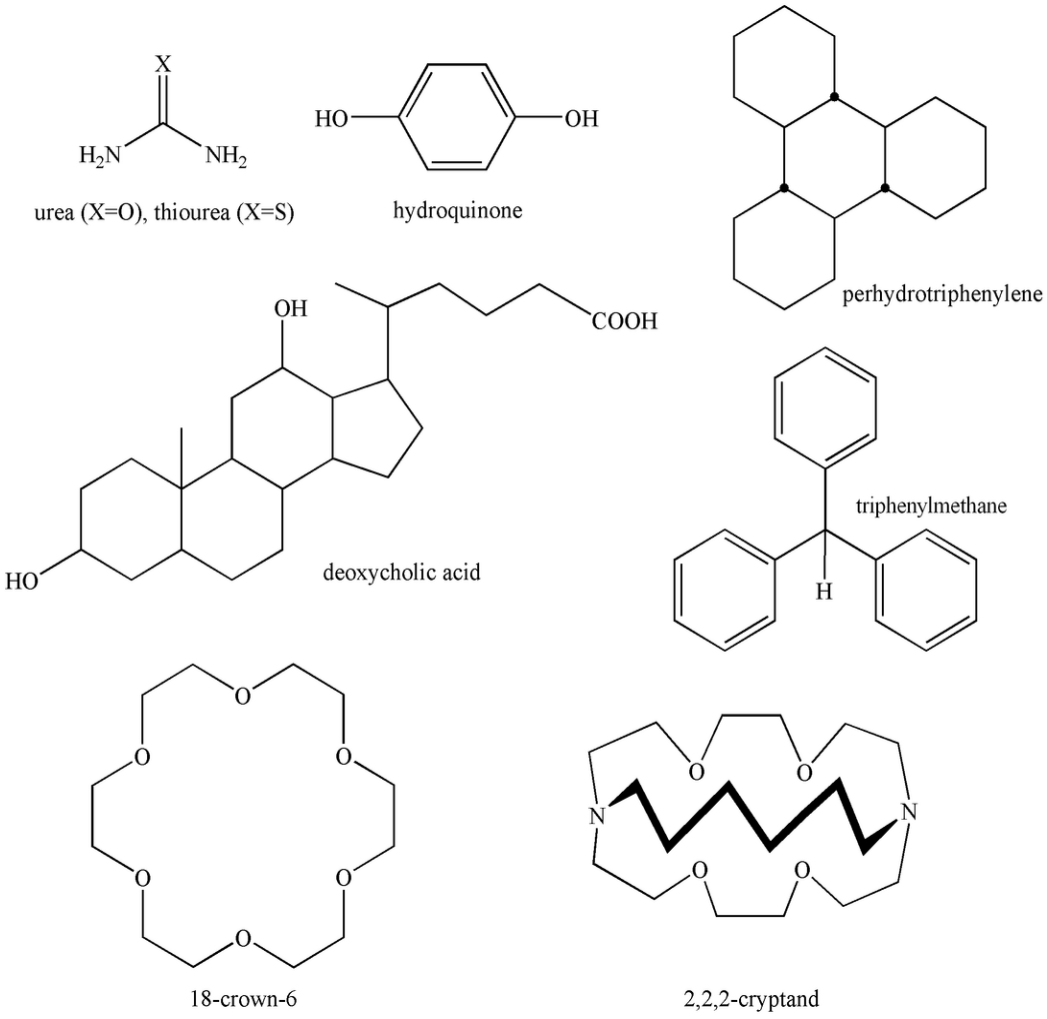

Figure 2 Chemical structures of organic host molecules[54]

Although a list of host molecule choices have been presented above, most literature dealing with the inclusion of long-chain polymers and the properties of the resultant polymer materials are actually narrowed down to the choice of cyclodextrin and urea, partially due to the ease of production of both materials. In the following sections, cyclodextrin and urea inclusion compounds will be discussed in detail.

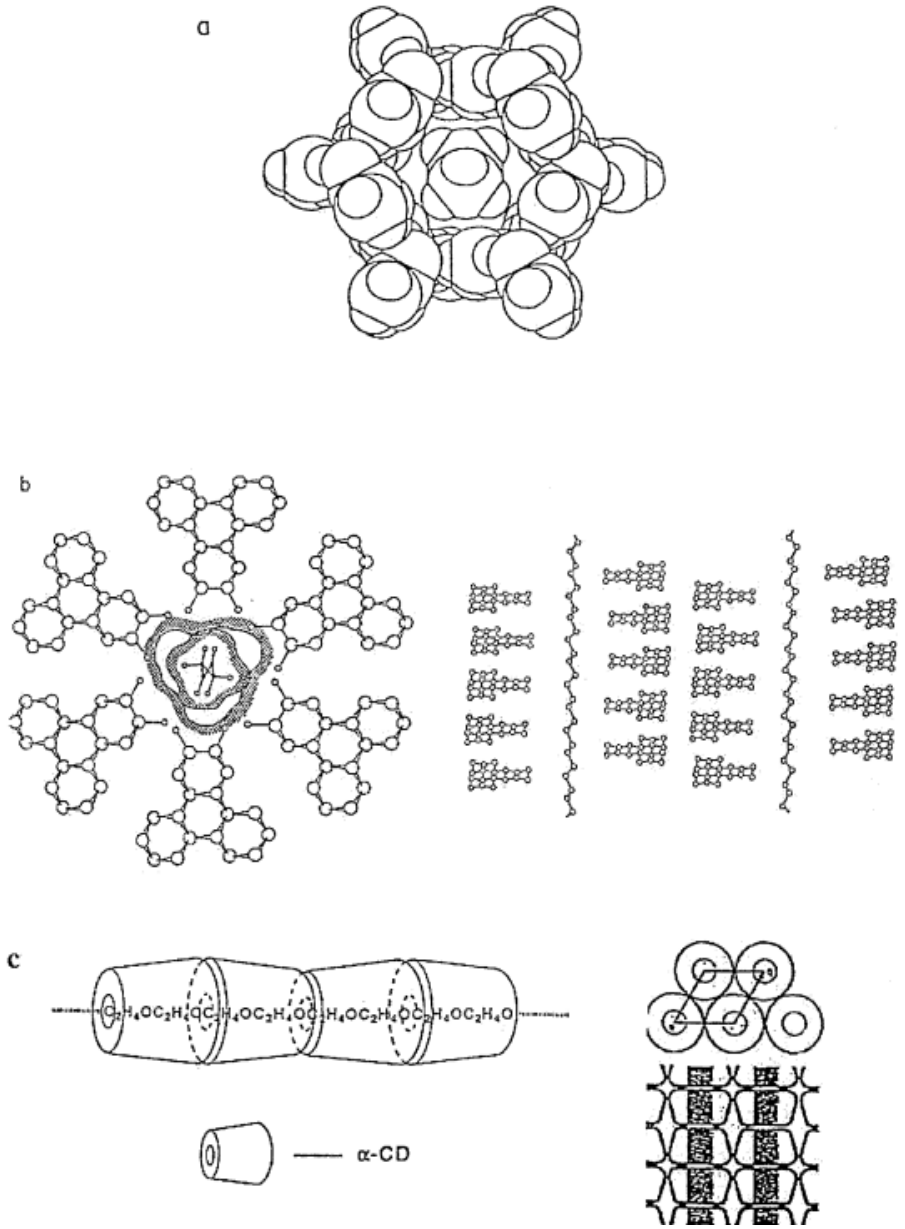

Figure 3 Polymer ICs formed between (a) polyethylene and urea, (b) trans-1,4-polybutadiene and perhydrotriphenylene, and (c) poly(ethylene oxide) and α-CD[44]

1.2.3 Cyclodextrin-Polymer Inclusion Compounds (CD-P-IC)

Cyclodextrins (CDs), also called cycloamyloses, are a family of cyclic starch derivatives which were first discovered by the French microbiologist A. Villiers in 1891 and were named as cellulosine due to its similar properties to cellulose.[55] In 1903, Austrian microbiologist F. Schardinger isolated two crystalline compounds, which were later named as α-dextrin and β-dextrin, from bacterial digestion of potato starch and suggested that they were identical to Villiers' cellulosine.[56] Schardinger continued this study and found that these compounds can be produced from different sources of starch using different bacteria.[57] Freudenberg and colleagues then suggested a cyclic structure for 'Schardinger dextrin', and therefore named it cyclodextrin. During that period, they also discovered γ-cyclodextrin, which has a larger ring structure. [58-60] Since then these three industrially produced cyclodextrins have been intensively studied for their structures, properties, and applications.

Though back in 1930s Pringsheim had already pointed out that these cyclodextrins tend to form complexes with a wide range of organic compounds,[61] it was not until 1990 that their ability to form inclusion compounds with guest polymers was discovered. Harada and Kamachi first demonstrated this new perspective by threading guest poly(ethylene oxide) (PEO) oligomers through the cyclodextrin (CD) cavities to form polymer threaded crystalline inclusion compound (IC).[62] Since then, a large number of crystalline CD-ICs have been formed containing either high molecular weight guest polymers or small molecule additives.[63]

1.2.3.1 Structures of CDs

In order to elucidate the mechanism of the cyclodextrin inclusion process, a detail understanding of their structures is necessary. The most common varieties are α, β, and γ- CD containing 6, 7, and 8 glucose units. (See Figure 4 below)

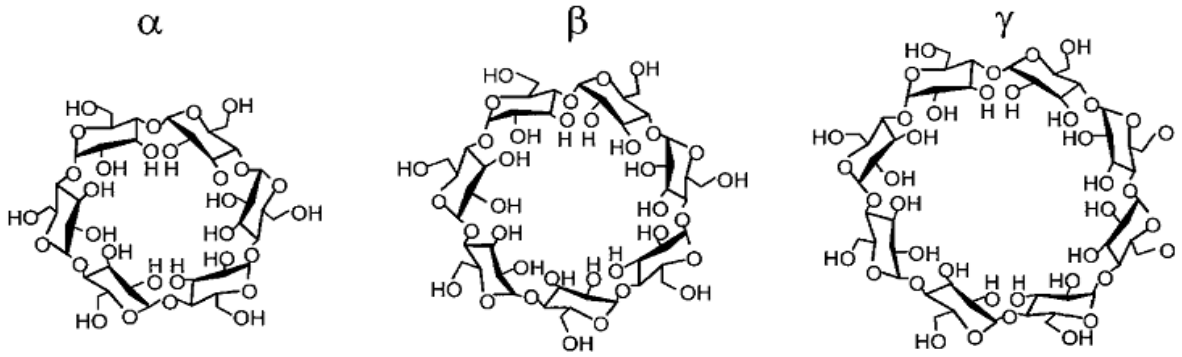

Figure 4 Chemical structure of α, β, and γ- CD [64]

All of them have truncated conical cylinder shape geometries, with primary hydroxyl groups on the narrow rim side and secondary hydroxyl groups on the wide rim side. They have internal cavities ranging from 0.5-1nm in diameter and the same height of 0.78nm. (See Figure 5 (b))

The total of 18-24 hydroxyl groups on the rims render cyclodextrin water soluble, while the inner cavities containing aliphatic entities have hydrophobic properties. (See Figure 6) Their dimensions as well as solubility data are listed in Table 1.

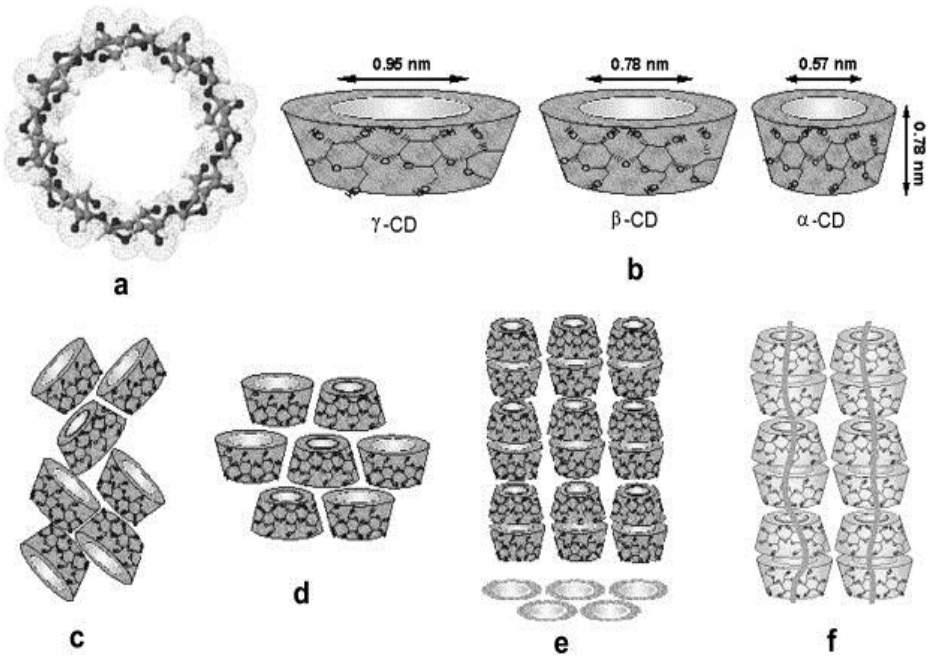

Figure 5 Structures of cyclodextrin: (a) γ-CD; (b) dimensions of α-, β-, and γ-CDs; schematic representation of (c) cage-type, (d) layer-type, and (e) head-to-tail channel-type CD crystals; and (f) CD-IC channels containing included polymer guests. [63]

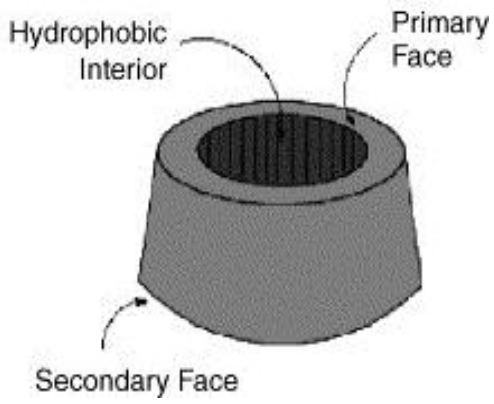

Figure 6 Schematic drawing of CD geometry[65]

Table 1 Characteristics of Cyclodextrins[65, 66]

Property	α-Cyclodextrin	β-Cyclodextrin	γ-Cyclodextrin
Number of glucopyranose units	6	7	8
Molecular weight (g/mol)	972	1135	1297
Solubility in water at 25 °C	14.5 (%, w/v)	1.85 (%, w/v)	23.2 (%, w/v)
Outer diameter (Å)	14.6	15.4	17.5
Cavity diameter (Å)	4.7–5.3	6.0–6.5	7.5–8.3
Height of torus (Å)	7.9	7.9	7.9
Cavity volume ($Å^3$)	174	262	427
Crystal forms (from water)	Hexagonal plates	monoclinic parallelograms	quadratic prisms

1.2.3.2 Nano-threading of Polymers into CD

There are two general considerations for the complexation of CD with guest molecules; the first would be the relative size between the cyclodextrin and guest molecule, and the second is the existence of a favorable net energetic driving force for the complexation process.[65] For example, the aromatic polyester poly (ethylene terephthalate) (PET) can only be included in the ~1.0nm channels of its γ-CD-IC, while the aliphatic polyester PCL can be included both in its ~0.6nm α-CD-IC as single chains and in the larger diameter γ-CD-IC as two parallel chains.[67, 68] As we can imagine, CD cavities should have stereoselectivity over guest polymer chains. In Shuai's work,[69] isotactic and atactic poly(3-hydroxybutyrates)s (i-PHB and a-PHB) were used as guest polymers to form inclusion compound with α, β, γ-CDs. It was found that the narrow i-PHB chain only formed inclusion compound with α-CD due to the too large cavities of β and γ CD for a tight-packing. The much wider conformations available to a-PHB, however, can only fit into γ-CD.

On the other hand, the thermodynamic driving forces for the complexation include the followings, owing to its unique amphipathic nature: first, the expelling of polar water molecules form the hydrophobic cyclodextrin cavity; second, the increased number of hydrogen bonds formed, as the water is expelled out of the cavity and have more access to form hydrogen bonds; third, as a non-polar guest is included into the cavities, its repulsive interaction with aqueous environment is reduced; fourth, favorable interactions between hydrophobic guest and internal cavities of CD are increased.[65]

Besides, it was determined that CD showed a preference for the inclusion of longer, higher

molecular weight polymers. It was suggested that this was mainly due to the slower unthreading of long polymer chain partially threaded with CDs compared to the rate of unthreading of a short chain.

1.2.3.3 Crystalline Structures of Polymer-CD-ICs

Cyclodextrins tend to adopt cage-type, or less often layer-type, crystalline structures (see fig. 1.5 c) when crystallized from water as hydrates or with the presence of small guests. However, under certain conditions, α and γ-CD can be recrystallized from water in a columnar channel structure, which resemble those of CD-plymer-ICs.[70] (see fig. 1.5 e and f, respectively) The inclusion of longer polymer chain make CD cavities line up and form long channels. Because of their unique crystal structure, which can be readily distinguished from their X-ray diffraction patterns, the formation of CD-polymer-ICs is easily confirmed.

1.2.3.4 Properties of guest polymers coalesced from polymer-CD-ICs.

Since polymer chains are threaded into and confined in such columnar long channels, it is reasonable to expect extended and isolated polymer chain within them. If CD hosts are carefully removed and guest polymer chains are allowed to coalesce into a bulk solid sample, the resultant extended, un-entangled and closely packed polymer chains should result in elevated physical properties compared to those produced from solution or melt. (See Figure 7 for schematic representation of the nano-structuring process)

After careful removal of CD from its polymer-CD-IC, using either enzymes or acids, coalesced crystallizable polymers evidence increased melting and crystallization

temperatures, while amorphous polymer show higher glass-transition temperatures.[71] It is more evident to see distinct morphologies for normally slow crystallizing polymers, such as PET. In Figure 8, coalesced PET film has more uniformly distributed and much smaller crystallites compared to the typical as-received PET film, which has larger spherulites size and a lower nucleation density.

The improved properties of polymer coalesced from their CD-ICs have been confirmed numerous times by Tonelli's group. The first known work on completely coalesced PCL was done by Wei et al.[73] in 2003, where PCL-α-CD-IC was coalesced using alpha-amylase enzyme from Bacillus licheniformis. The coalescence was confirmed via absence of a characteristic band for α-CD in the FTIR spectrum of the coalesced sample, which is roughly identical to that of the as-received PCL. The melt-crystallization was studied by both isothermal and non-isothermal crystallization, and the Avrami exponent (n) was determined to be close to 4, which is an indication of homogeneous crystallization. Due to the low yield of coalesced polymer, the resultant properties, other than thermal, had not been investigated until Williamson's[5] work was published. Williamson et al. employed both enzyme and acid wash coalescence and found that the acid wash was much more efficient than enzyme wash as evidenced by the comparison of FTIR spectra for them. (See Figure 9) Acid-washed samples have no characteristic band peak for α-CD around 3000-3500 cm^{-1}. Relative effectiveness of coalescence methods were also determined and are listed in Table 2 below.

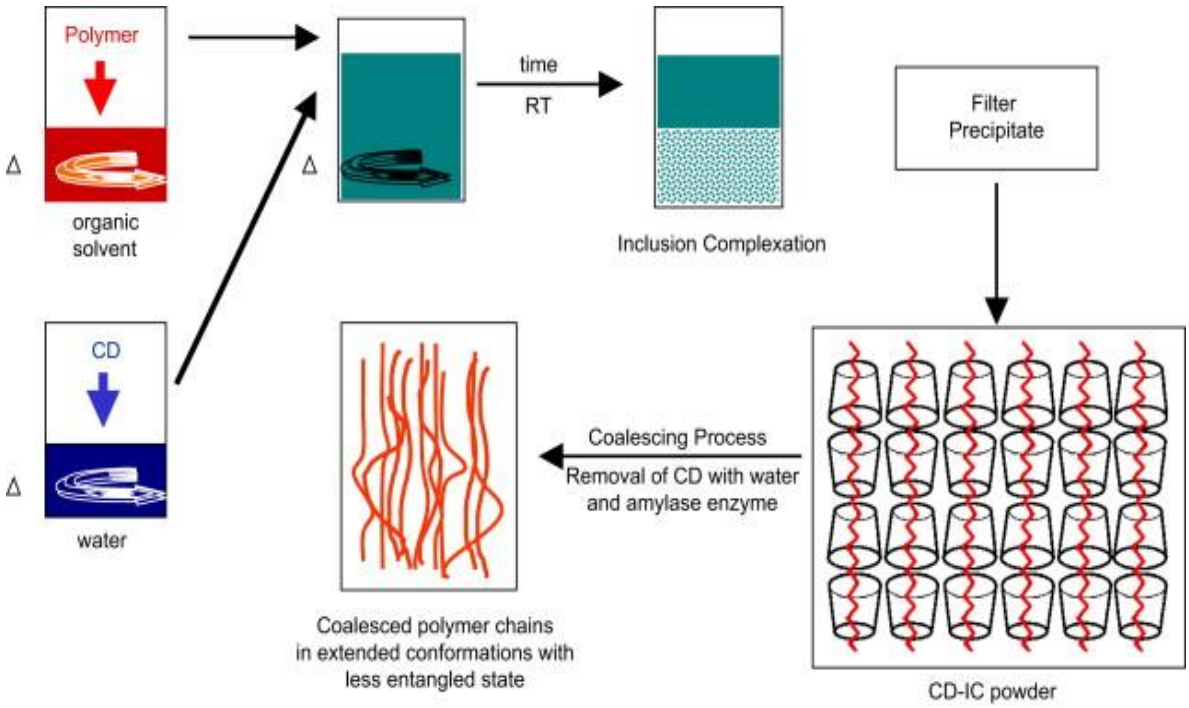

Figure 7 Schematic representation of polymer–CD-IC formation, the coalescence process, and the coalesced polymer[50]

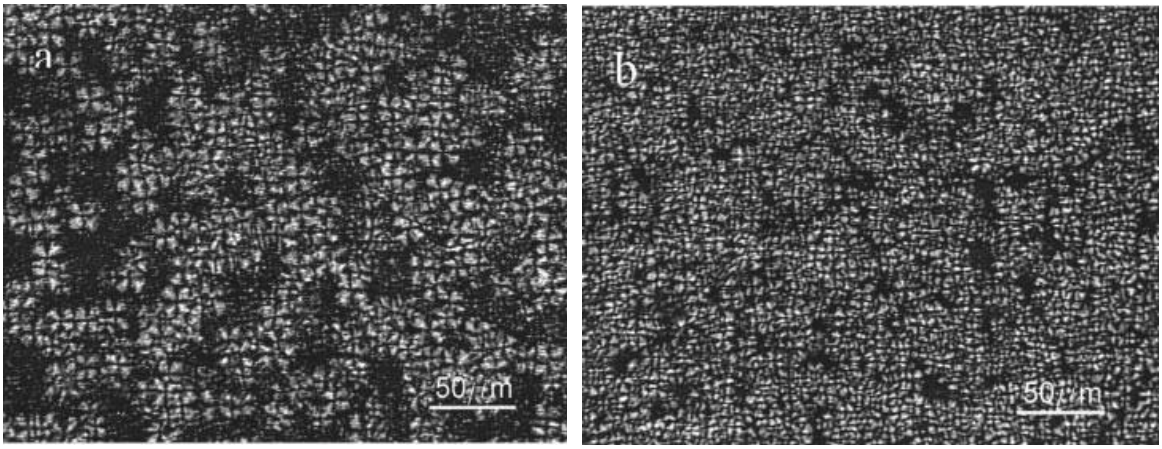

Figure 8 Polarized light micrographs of melt-crystallized (a) as-received PET and (b) coalesced PET[72]

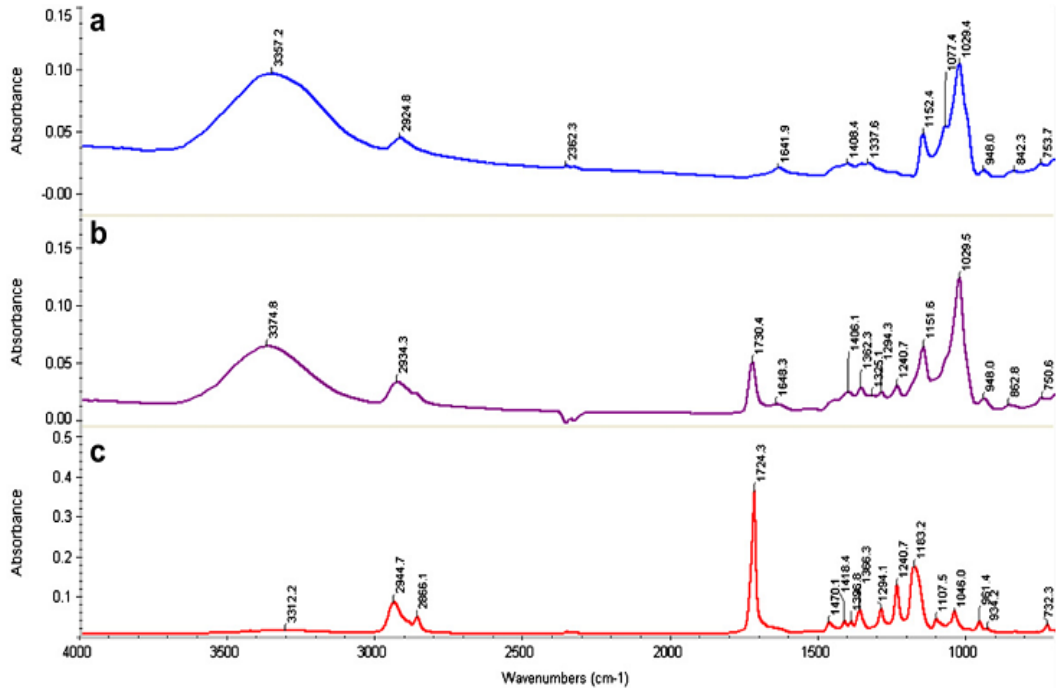

Figure 9 FTIR spectra of α-CD (a), PCL-a-CD-IC enzymatically washed (b), and HCl-coalesced (c) [5]

Table 2 Percentage of Remaining a-CD after Various Coalescence Techniques[5]

Coalescing technique	Estimated remaining CD (%)
Hot water washing	17.8
Enzyme washing	12.7
Soxhlet extraction	12.6
Acid washing	Trace

The densities of as-received and completely acid-washed coalesced PCLs were determined by floatation. An increase of 3% in density of the amorphous regions was estimated and indicates a closer packing of polymer chains in the non-crystalline regions of the coalesced sample. Dynamic Mechanical Analysis showed that coalesced PCL was more elastic than as-received PCL. Nanoindentation showed an increase of 33% in hardness and 53% in Young's modulus for coalesced PCL film as compared to as-received PCL film. However, there was still not enough coalesced sample to perform tensile tests on these materials.

1.2.3.5 Problems with CD

Although this manner of nanoprocessing polymers has been shown to significantly alter their behaviors, the tedious coalescence process hinders the pace of its application. First of all, even after taking a very long time to remove the threaded cyclodextrin, the effectiveness is still not ensured. (see table 1.2) The second consideration is whether a small amount of cyclodextrin remains and affects the improved melt-crystallization and physical properties of coalesced polymer, which is believed to be the consequence of their coalesced conformations, structures, and morphologies. If the problem of remnant threaded CD can be bypassed and yet still achieve similar improvement in their ability to crystallize from their melt, even after spending a long time above their melting temperature, the suggested explanation can be confirmed. In the light of this, we recall that the inclusion compounds formed between small molecule hosts and polymers have the similar function of isolation and extension of random coiling polymer long chains and that the host small molecules are just packing around the polymer chains instead of threading, as is the case of CD-ICs. This type of inclusion

compound can easily be deconstructed and the host readily removed, insuring an alternative and easier method of nano-processing polymers.

1.2.4 Urea Inclusion Compounds (U-ICs)

Urea is such a small host molecule that can form channel structures in which polymer chains are included. In 1940, the first urea inclusion compound was discovered by Bengen[74]who accidently found that 1-octanol and urea formed a crystalline adduct. Many other different guest molecules were subsequently investigated and found to form inclusion compounds with urea. Smith[75] applied X-ray diffraction to the study of crystalline inclusion compounds formed between hexadecane and urea.

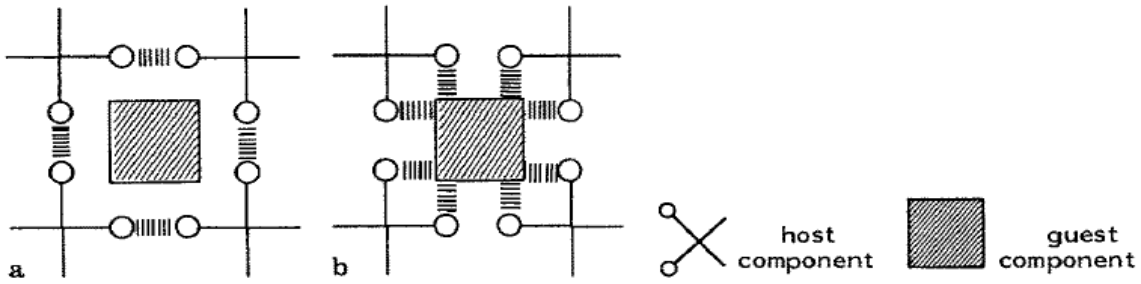

Figure 10 Different modes of lattice inclusions: (a) cross-linked matrix type of inclusion (b) coordinate-clathrate type of inclusion[77]

The crystalline structure of the inclusion compound formed between hydrocarbons and urea were found to be hexagonal tunnel structures, which are constructed by extensively hydrogen-bonded urea molecules, with no coordination between urea and guest molecules.

They were characterized as “true clathrates” for forming channel structures with only host molecules themselves.[76] (See Figure 10)

1.2.4.1 Formation of the Crystalline Matrix

An over-simplified description of how inclusion compounds were formed from their solution stated that a suitable nucleus present in a supersaturated solution triggers crystallization.[78] The crystallization process can also be regarded as two separate steps; first the host molecules form an unstable structure with empty cavities, and second the geometrically compatible guest molecules thread into the cavities and stabilize the unstable structure, which is not available for pure host crystal. For comparison, urea itself crystallized from solvent is a closely packed tetragonal crystalline structure.[78] The majority of inclusion compounds formed with linear molecules and urea were found to adopt honey-comb networks, containing linear parallel helical channels with effective diameters ranging from 5.5 to 5.9 Å, as long as the requirements for critical minimum chain length and limited branching are met. (See Figure 11) Another type of host molecule, thiourea, forms similar honey-comb structures which are not helical and have larger channel diameters ranging between 5.8 and 7.1 Å. Analogous to the fact that three different size cyclodextrins accommodate different types of polymers based mainly on their sizes, thiourea inclusion compounds have larger channel diameters adequate to include some branched polymer chains, which cannot be included in the conventional hexagonal urea channels.[79] The size and shape selectivity of the crystalline structures lead to the applications in molecular separation, e.g., in the petrochemical industry. In addition, the chiral characteristic of urea inclusion compounds was

also used to separate enantiomers.[80]

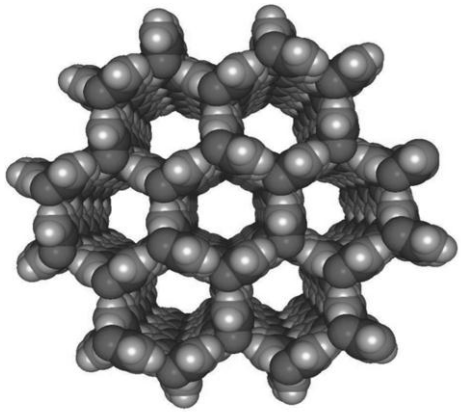

Figure 11 Perspective view along the channel axis of the honeycomb host network in an urea inclusion compound[79]

1.2.4.2 Polymer-U-ICs

Urea inclusion compounds formed with long polymer chains are usually prepared by co-crystallization from a combined solution, where the host and guest molecules are dissolved or from their melt mixture. The polymer chains confined in the narrow channels in general prefer to adopt essentially the all-trans conformation. PE adopted all-trans conformation without any sign of the presence of gauche conformations or rotational interconversion between them, and poly(ethylene oxide) (POE) adopted conformations considerably more extended than that adopted in the crystal of pure POE.[27] Both nylon-6 and PCL are able to adopt only five distinct conformations which have sizes appropriate for the channel formed by urea with other polymers (5.25-5.5 Å). Those conformations include the all-trans, planar

zigzag conformation, and four kink conformers with g $^{+/-}$ t g $^{-/+}$ sequences. However, it was determined by modeling that it is not possible for them to interconvert with each other without unthreading part of the chain out of the channel.[28] Stereoregular poly(L-lactide) (PLLA) in the extended, nearly planar zigzag, all trans conformation fit in the channel, while regularly alternating poly(L,D-lactide) did not.[33] Some common polymers and their urea inclusion compound structures are listed in Table 3.

The extension of polymer chain conformations is the key of our nanostructuring process, which is similar to what has been achieved in CD-ICs. Due to the unstable nature of the empty host urea channel structure, which soon collapses after the included guest molecules have been removed, it is extremely easy to extract the polymer from its U-IC as compared to the coalescence from its CD-IC. The flow diagram of nanostrcuturing polymer chains with urea inclusion compounds is depicted below. (See Figure 12) This idea of recovery from its U-IC by extraction with a non-solvent for polymer was proposed by Vasanthan et al.[35] in 1994. DSC observations showed that IC-recovered PCL produces crystals that melt 6 ℃ higher than PCL recrystallized from solution or the melt. Extended chain morphology was believed to be the cause of the change in crystallization process. FTIR and NMR observation indicated a similar extended, nearly all-trans conformation for PCL chains in the PCL-U-IC and in the bulk. However, there was no further investigation of its physical properties.

Table 3 Urea Inclusion Compounds with Various Guest Polymers and Their Structures

Guest Molecules	Tm(° C)	Crystal Structure	References
Poly(ethylene oxide)	143	trigonal(solution) hexagonal(melt)	81
Poly(tetrahydrofuran)	135–138	hexagonal	82
Poly(ethylene)	148	hexagonal	75
Poly(ε-caprolactone)	142	hexagonal	83
Poly(L-lactic acid)	137	hexagonal	84
Poly(1,3-butadiene)	123–128	hexagonal	85
Polypropylenes	138	large tetragonal	86
Poly(acrylonitrile)	–	pseudo-hexagonal (or large tetragonal)	87

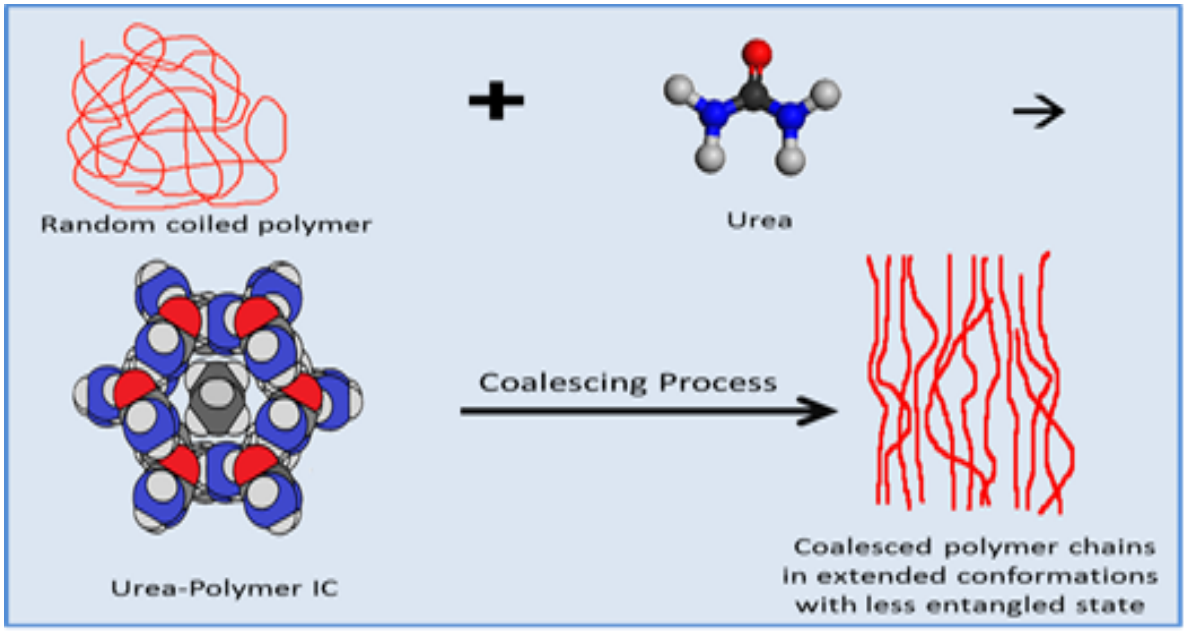

Figure 12 Schematic representation of polymer–U-IC formation, the coalescence process, and the coalesced polymer

1.3 Coalesced PCL as a Self-nucleating Agent

Nucleating agents are often utilized to control nucleation density, spherulite size and distribution, and therefore improve the physical properties of melt-crystallized polymers. Heterogeneous nucleating agents, which are insoluble in the polymer melt, are often used in industrial processing. However, in the sense of improving the physical properties of a polymer material which targets the bio-medical market, the nucleating agent must also be bio-absorbable and nontoxic. Gurarslan[88] found nylon-6 (c-N-6) coalesced from N-6-α-CD-IC crystals at low concentrations to serve as an effective self-nucleating agent for the bulk crystallization of N-6 from the melt. Williamson[5] evaluated the ability of PCL coalesced from

its α-CD-IC to act as a self-nucleating agent. It was also found to effectively nucleate the melt-crystallization of as-received PCL. This homogenous self-nucleating agent is not only non-toxic and biodegradable, but also chemically compatible with the as-received material. The discussion of the effectiveness of polymers coalesced from their U-IC acting as self-nucleating agents remains to be done in the current work.

1.4 Motivation

PCL has excellent bio-compatibility and bio-degradability, while it is not a strong material for load bearing biomedical applications. However, if it is possible to maintain its unique properties and increase its physical strength without changing its chemistry, PCL will no doubt be the most promising material in the biomedical industry. Endeavors have been made to nano-process it with cyclodextrin, and a positive result has been obtained. In order to bypass the tedious coalescence process from CD-IC, we propose to use another small molecule host (urea) to form crystalline channel matrix which can be readily removed by stirring in a non-solvent for the polymer. The work discussed in the following chapters is committed to systematically test the feasibility of the procedure and the performance of the resultant coalesced polymer is compared to that processed from cyclodextrin.

Chapter 2: Experimental

2.1 Materials

Four samples of poly(ε-caprolactone) having number average molecular weights of 80,000, 42,500, 10,000, and 2,000 g/mol (asr-PCL-80,-40, -10, and -2) (See Table 4) were obtained from Sigma-Aldrich, as were acetone, methanol, and urea. It should be noted that each PCL contains a centrally located –(CH_2-CH_2-O-CH_2-CH_2-)– unit, as shown below. As a consequence, the two connected PCL chains run in opposite directions.

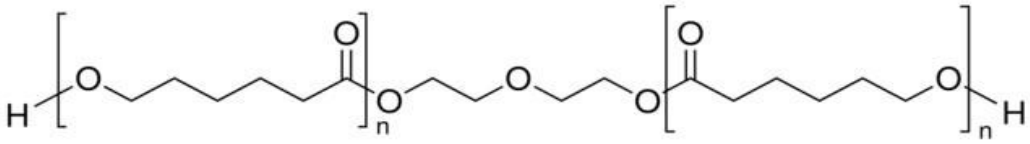

Table 4 PCL Samples

Sample ID	Commercial Name	M_n (g/mol)*	n
PCL-2	**Polycaprolactone diol 189421**	**2,000**	**8**
PCL-10	**Polycaprolactone 440752**	**10,000**	**43**
PCL-40	**Polycaprolactone 181609**	**42,500**	**186**
PCL-80	**Polycaprolactone 440744**	**70-90,000**	**350**

*Provided by the manufacturer.

2.2 Methods

2.2.1 Formation of PCL-U-ICs

1 g of PCL was dissolved in 120 ml of acetone at 50° C, and 14 g of urea (U) were dissolved in 70 ml of methanol also at 50° C, and the U solution was slowly added to the PCL solution in a drop-wise manner. The temperature was lowered after mixing was complete, but stirring continued at room temperature for an additional 30 min. A further two days were allowed for inclusion complex formation, after which the resulting precipitate was filtered and vacuum dried.

2.2.2 Coalescence of PCL from its U-IC

Urea can be removed from the PCL-U-IC by two techniques. Stirring 1 g of PCL-urea-IC in 50 ml of methanol can completely remove the U. In a second route, 1 g of PCL-urea-IC was stirred in excess water for one day and then filtered and dried. Then 1 g of the resulting material was stirred in 35 ml of methanol to completely remove the U and obtain coalesced PCL. Though the second route takes longer, it requires less methanol. Finally, in both cases the coalesced PCL samples were vacuum dried for one day. The yield in terms of PCL from the as-received sample to coalesced sample was ca. 60%.

2.2.3 PCL Films

Solvent cast PCL films were obtained by dissolving 1 g of PCL in 100 ml of acetone and then evaporating all the solvent. PCL films nucleated with c-PCL were obtained by solvent

casting of 2.5 % c-PCL with 97.5 % as-received (asr)-PCL from acetone, which did not dissolve the c-PCL nucleant. All solvent-cast films were vacuum dried before further characterization. Melt pressed films of asr and c-PCL were prepared for polarized microscopy, tensile testing, nanoindentation, and density determination.

2.2.4 Long Time Annealing Study

c-PCL samples were kept in the oven above their melting temperature (T_m) at 80 ℃ for 3 days, 2 weeks and 4 weeks to determine the thermal stability of coalesced materials. DSC was performed at each interval to see if their improved melt-crystallization behavior was retained after being kept in the melt state for a long period of time.

2.3 Characterization

2.3.1 FTIR

Fourier Transform Infrared Spectroscopy (FTIR) analysis was performed on a Nicolet Nexus 470 Spectrometer in the range 4000 - 400 cm^{-1}, with a resolution of 4 cm^{-1}. A Nicolet OMNI Germanium Crystal ATR sampling head was employed. 64 scans of data were collected and analyzed for each sample by using Omnic software.

2.3.2 DSC

Differential scanning calorimetric (DSC) thermal scans were performed with a Perkin Elmer Diamond DSC-7 instrument. Heating scans were started at 0° C, and each sample was heated to 75° C. After holding each sample in the melt for 5 min, they were cooled to 0° C at the

same rate they were previously heated (20° C/min). Nitrogen was used as the purge gas. DSC data were analyzed with Pyris software and melting and crystallization temperatures and enthalpies were calculated automatically by the software from the areas of their endothermic and exothermic peaks.

2.3.3 Polarized Microscopy

Polarized optical microscopic observations of as-received and coalesced PCL thin films were performed on a Nikon Eclipse 50i POL Optical Microscope equipped with a CCID-IRIS/RGB color video camera made by Sony Corp. Photographs were taken by using crossed polarizers and a ¼ λ plate.

2.3.4 NMR

Dilute solutions of c-PCL and a mixture of 10 wt% urea and 90 wt% asr-PCL were prepared in 1:2 d_6-DMSO:$CDCl_3$ mixtures and their ^{1}H-NMR spectra recorded on a Bruker 700Mhz spectrometer equipped with a 5 mm ID CPTCI (^{1}H/^{13}C/^{15}N/D) Z-Axis Gradient cryo probe. NMR data were analyzed with Topspin 2.1 software.

2.3.5 XRD

X-ray diffraction analysis was done using a Philips XLF, ATPS X-ray diffractometer with an OMNI Instruments customized auto-mount and copper tube. The tube produces X-rays with a wavelength of 1.54Å. The diffractograms were obtained over a 2θ range of 5-50^{o}. The data was analyzed using TXRD 5.1 software.

2.3.6 Flow Time Measurement

Flow times for both as-received and coalesced PCL 80,000 were measured with a #50 Cannon-Ubbelohde viscometer. Each sample was weighed to ~0.25 gram with the maximum possible precision and dissolved in 30ml of acetone in a capped conical flask with mild heat and stirring applied. The solutions were then transferred to 50ml volumetric flasks. All the glassware in contact with solution were rinsed with acetone and transferred to the volumetric flasks. Then pure acetone was added drop-wise to the volumetric flasks until they reached the indicated 50ml marks. The solutions were mixed thoroughly after capping with a glass stopper, achieving concentrations of 0.5g/dL.

Rinse the viscometer with acetone several times and record the flow time of pure acetone before measuring each sample solution. Each sample was measured at least 3 times and the average flow time was taken.

2.4 Physical Properties

2.4.1 Tensile Tests

Tensile tests were conducted according to ASTM D-882-02 using a MTS Q-Test™/5, CRE-type tester. The test specimens were prepared by cutting 0.30-0.42 mm thick films into 6mm wide and 90 mm long dog bone shapes using a template.(See Figure 13) Tensile tests were

performed using a 250 lb load cell, and the gauge length was 50mm. The cross-head speed was 500 mm/min. Modulus values were calculated from the slope of the initial part of the load-elongation curve where the slope is constant. According to ASTM D-882-02, a minimum of five specimens of our PCL films were tested from each sample. Specimens that failed at some obvious flaw or slip from the clamp were discarded and retests made.

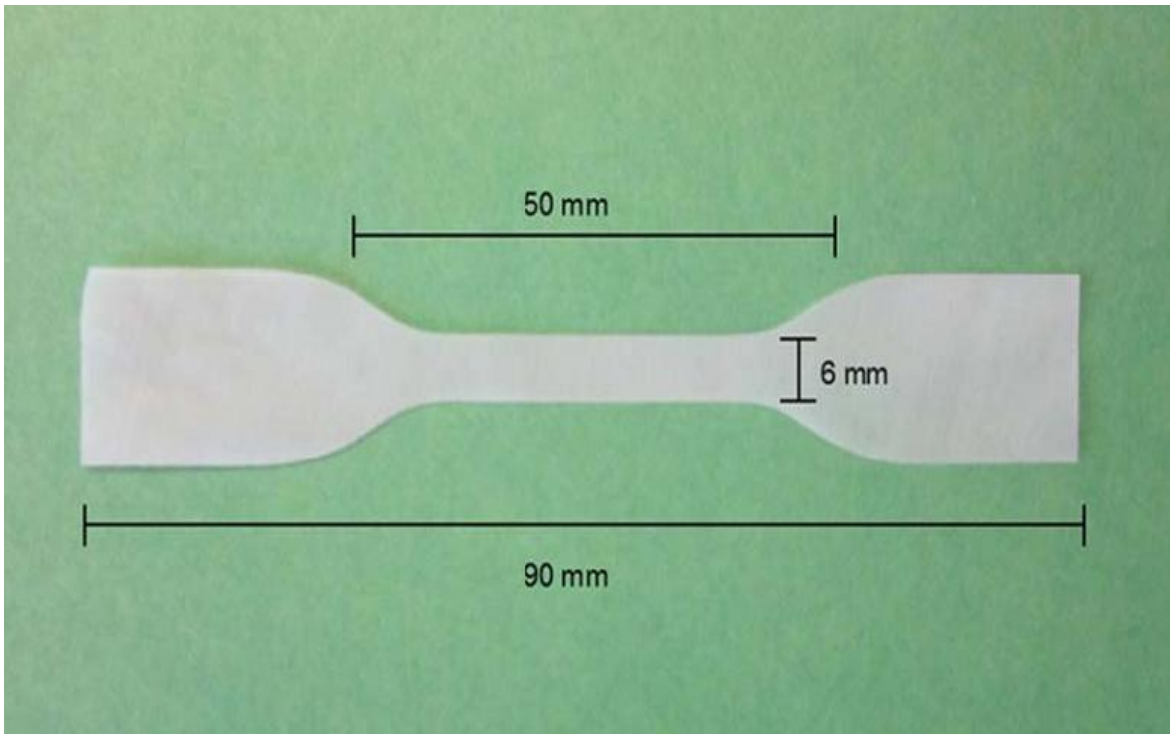

Figure 13 Dog-bone shape PCL film specimen and their sizes[89]

2.4.2 Density Measurements

The densities of as-received and coalesced-PCL films were measured by floatation using deionized water and aqueous sodium bromide (NaBr) solution. The density of NaBr solutions

with respect to its solute wt% can be found in a handbook.[90] The high density 22wt% NaBr solution was added slowly using a burette to a premeasured volume of deionized water containing both PCL samples at the bottom. A stir bar was used to completely mix the solution. When the density of the aqueous salt solution matches the density of the sample, the sample reaches neutral buoyancy. The volumes of added NaBr solution for both as-received and coalesced-PCL at neutral buoyancy were noted respectively. The PCL sample density can be calculated by the following equation:

$$\rho_{sample} = \frac{vol(H_2O) \times \rho(H_2O) + vol(NaBr/H_2O) \times \rho(NaBr/H_2O)}{vol(H_2O) + vol(NaBr/H_2O)}$$

2.4.3 Nanoindentation

Nanoindentations were performed on PCL films using a Hysitron TriboIndenter and TriboScan software. All tests were performed at room temperature (~25˚C) on small 5mm by 5mm squares of melt pressed PCL films (~0.4 mm thick). Four points in a 2×2 square pattern were selected for each sample and each point was indented 4 times separately with four different predetermined maximum forces (500μN, 1000μN, 1500μN, and 2000μN) using a Berkovich tip. (See Figure 14)

The software recorded the force as a function of displacement and the loading and unloading

curve was obtained for each indentation. (See Figure 15) Then the hardness and reduced modulus values were determined automatically by the software from the loading and unloading curves. Topographic visualizations of the indented film can also be collected using the Hysitron hardware and software. (See Figure 16)

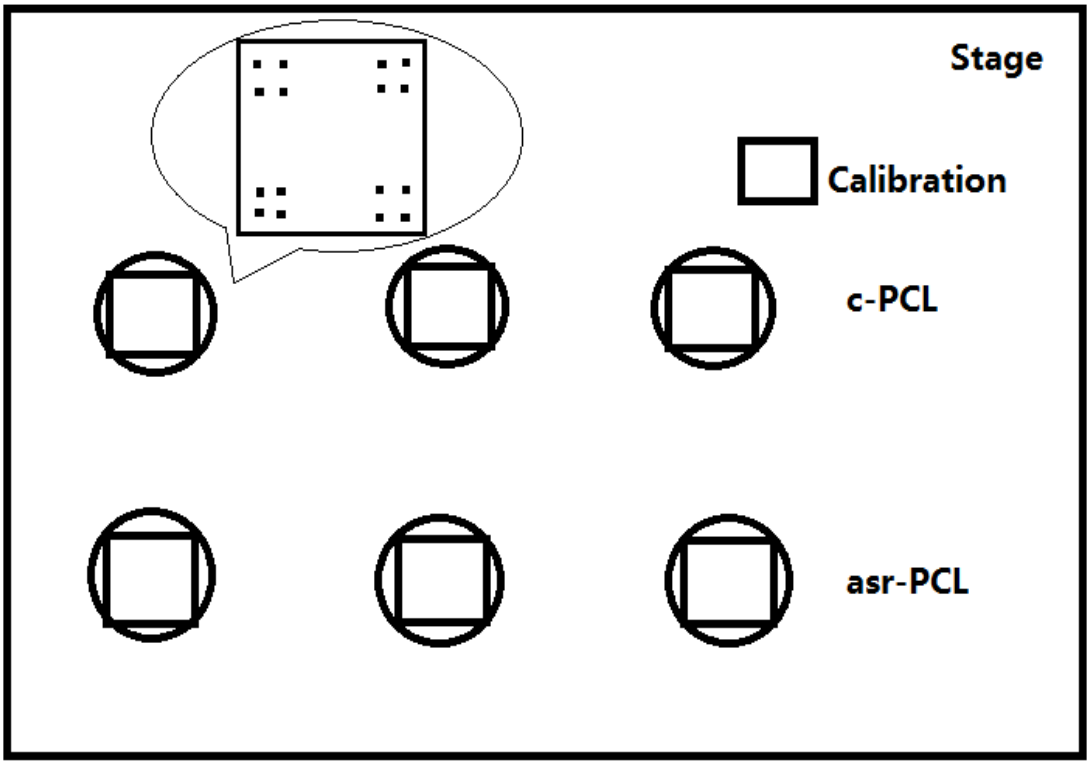

Figure 14 Schematic view of PCL samples and indentation positions.

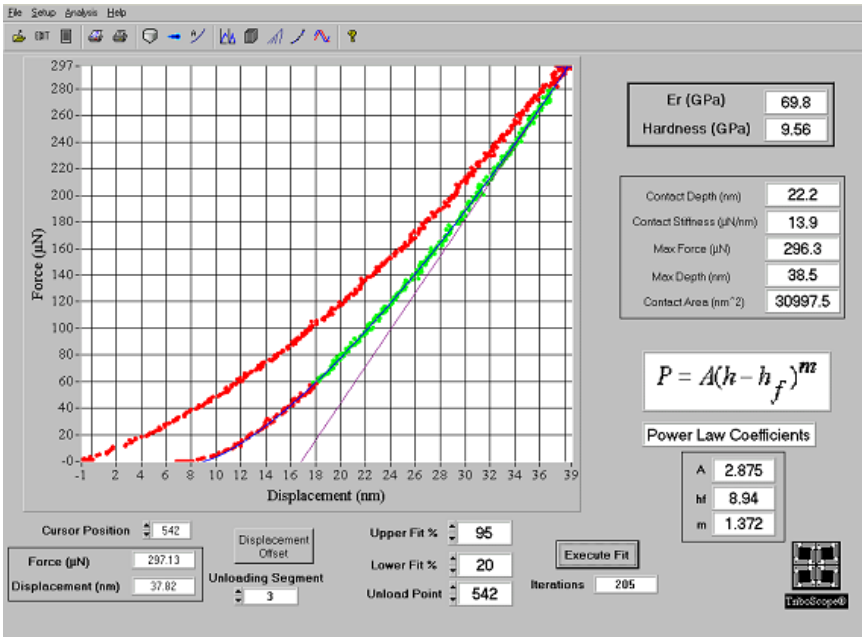

Figure 15 Example of a nanoindentation loading and unloading curve[91]

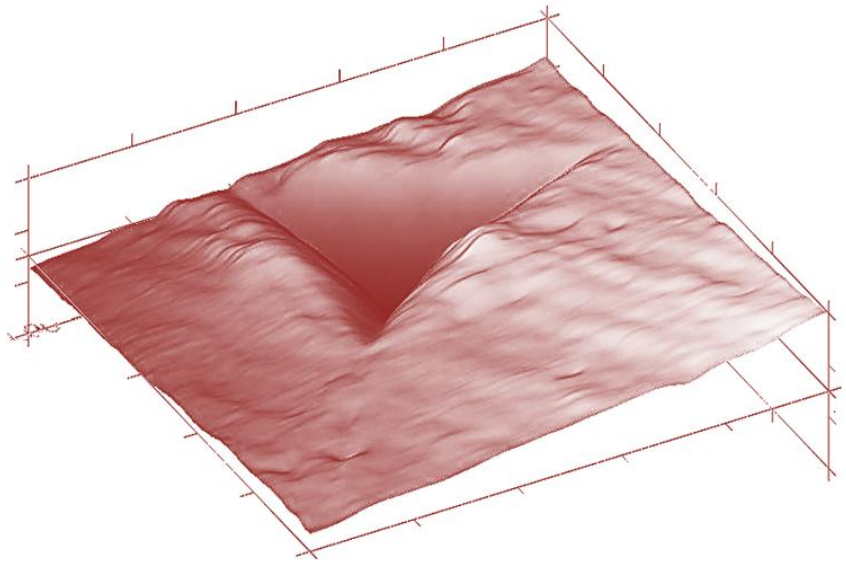

Figure 16 Topographical scan of the as-received PCL sample surface post-indent [92]

From the reduced modulus, which accounts for the elastic properties of both sample and diamond indenter, the Young's modulus of the sample can be calculated provided the Poisson's ratio for both diamond indenter and sample and the Young's modulus for diamond indenter are known. The equation assumes additivity of compliances:

$$\frac{1}{E_r} = \frac{(1-\nu^2)}{E} + \frac{(1-\nu_i^2)}{E_i}$$

in which,

E_r -Reduced Modulus (GPa)

E -Young's Modulus of PCL Sample (GPa)

v – Poisson's Ratio of PCL Sample

E_i –Young's Modulus of the Diamond Indenter (GPa)

v_i –Poisson's Ratio of Diamond Indenter

The Young's modulus and Poisson's ratio for diamond indenter are 1141 Gpa and 0.07, respectively.[93] The Poisson's ratio for semi-crystalline PCL in the literature is 0.46.[94] DSC results showed an equal amount of crystallinity for all PCL samples that have been sitting at room temperature for more than a day irrespective of the previous cooling profile. This is mainly due to the fact that its T_g is below room temperature, so 'annealing' was taking place. Provided that the crystallinities of our c-PCL and asr-PCL are similar and that minor

difference in the Poisson's ratio will not affect the Young's modulus of the sample,[95] it is reasonable to use 0.46 for both of them. Although the software did all the calculations except the conversion from reduced modulus to sample Young's modulus, close scrutiny of what the software does is necessary if we want to better interpret the results.

Doerner and Nix[95] first proposed in 1986 to relate the load and displacement data to contact area, which is assumed to be constant upon unloading, and therefore the indenter was modeled as a flat punch. In this method, only one cycle of loading and unloading is needed without the need to image the hardness impression. Once an area function is generated for the indentation performed by a specific indenter by measuring its replica under Transmission Electron Microscope (TEM), the contact depth can be successfully related to the contact area. The maximum load, P_{max}, the maximum displacement, h_{max}, elastic stiffness, S=dP/dh, which is determined from the derivative of the initial part, and the final depth, h_f, should be determined from the P-h curve.[93] To better estimate the contact depth, Oliver and Pharr[93] proposed an improved method that modeled the Berkovich indenter as a conical indenter. The elastic displacement of the periphery of the contact area, h_s, can be calculated by:

$$h_s = \epsilon \frac{P_{\max}}{S}$$

where, ε is an indenter geometry dependent constant and 0.75 is used as a standard value based on empirical observations. The relationship between those quantities used for analyzing the P-h data is illustrated in Figure 17, where the contact depth, h_c, can be

expressed as:

$$h_c = h_{max} - h_s = h_{max} - 0.75\frac{P_{max}}{S}$$

where *S* was determined from the slope of the P-h curve at the beginning of the unloading, h_{max}, and P_{max} were also determined from the curve. Once the contact depth is obtained, the contact area can be directly calculated from the area function determined by the method introduced by Doerner and Nix, and the hardness can be obtained from:

$$H = \frac{P_{max}}{A(hc)}$$

The reduced modulus, E_r, can be assessed using the following relationship:

$$S = \frac{dP}{dh} = \beta\frac{2\sqrt{A_{max}}}{\sqrt{\pi}}E_r$$

The dimensionless parameter β was originally taken as unity. However, recent research showed the importance of refinement, which accounts for all physical processes deviating from the relationship. [96]

In this way, the software calculates and outputs the hardness and the reduced modulus from the recorded P-h curve of the sample.

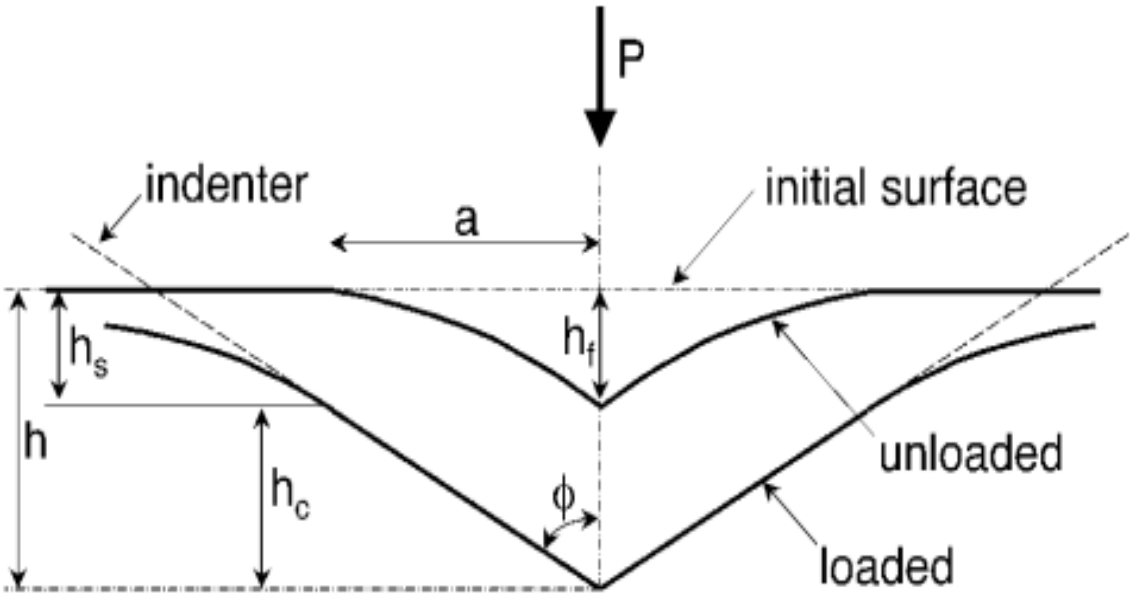

Figure 17 Schematic illustration of the unloading process showing parameters characterizing the contact geometry[96]

Chapter 3: Results and Discussions

3.1 Confirmation of IC formation

3.1.1 FTIR

FTIR spectra of PCL-U-ICs exhibit peaks characteristic of both PCL and U, indicating the co-existence of both components. (See Figure 18) That the vibrational peaks in the PCL-U-IC spectrum shift slightly from their original wavenumbers in pure PCL and pure U indicates potential interactions between the two components and the formation of new structures, *i.e.* PCL-U-IC.

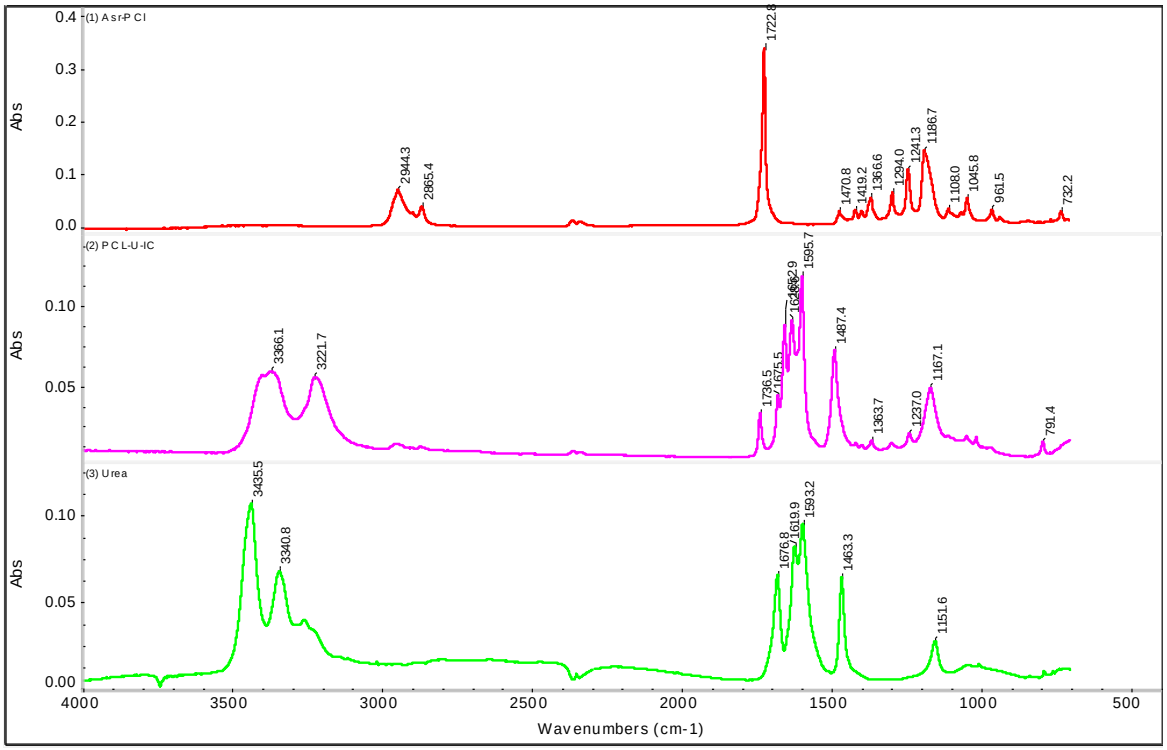

Figure 18 FTIR spectra of Asr-PCL (1), PCL-U-IC (2), and Urea (3)

U peaks between 3000 and 3500 cm^{-1}, that correspond to NH_2 stretch in the urea, showed a clear shift upon the formation of IC. PCL peaks in the IC at 2865 and 2944 cm^{-1}, that represent CH_2, did not change much from pure PCL. Because of the overlapping of PCL and U peaks between 1000 and 1800 cm^{-1}, spectra were expanded to more readily observe the multiple peaks in this range. (See Figure 19)

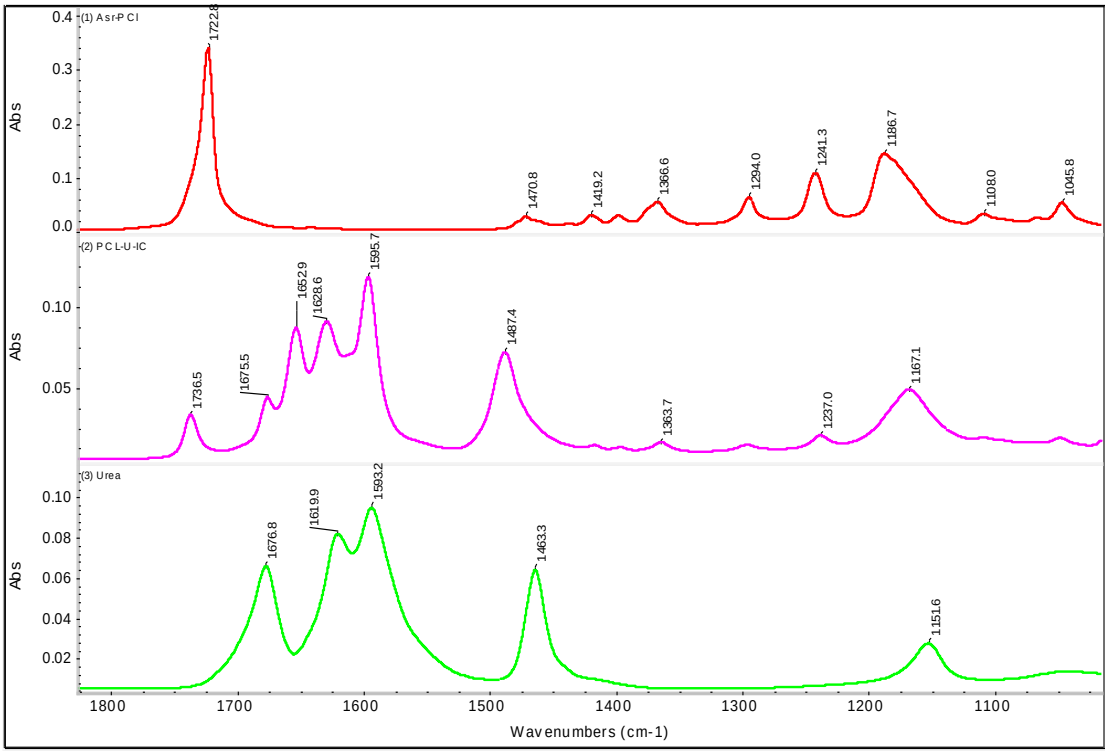

Figure 19 FTIR spectra between 1000 and 1800 cm-1 of Asr-PCL (1), PCL-U-IC (2), and Urea (3)

The carbonyl (C=O) stretch for PCL at 1723 cm^{-1} shifted to 1737 cm^{-1} when PCL chains were separately included in the hexagonal urea channels. Previous study by Vasanthan et al.[97]found a peak at 1724 cm^{-1} and a shoulder at 1738 cm^{-1} in semi-crystalline PCL sample

and assigned them to be the crystalline and amorphous contributions, respectively. This was initially proposed by Coleman et al.[98]who scanned FTIR spectrum for PCL above its melting point at ~75℃. (See Figure 20)

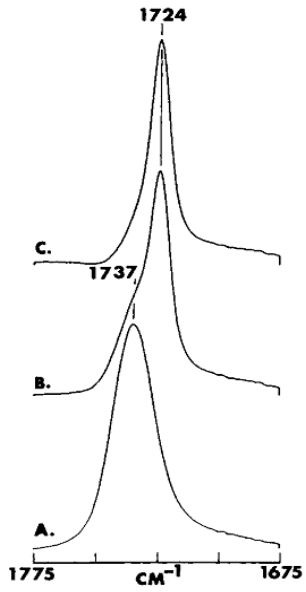

Figure 20 FTIR spectra in the range 1675-1775 cm-1. (A) Spectrum of PCL recorded at 75℃ (amorphous). (B) Spectrum of PCL aged for over one month and recorded at room temperature (semicrystalline). (C) Difference spectrum obtained by subtracting A from B. [98]

This made clear that carbonyl stretching in amorphous PCL is located at 1738 cm^{-1}, where that of our included PCL is also located. Certainly the PCL chains in the channel are not in the amorphous phase, which is believed to be randomly coiling without any order. Instead, it is believed to have extended and separated chains in the U-IC. The fact that PCL chains

adopt nearly all-trans conformations in their crystalline phase and that the channels are only able to accommodate extended conformations, nearly all-trans, planar zigzag, and four kink conformers, with $g^{+/-}$ t $g^{-/+}$ kink sequences, suggest the separation of the chains, not the extended conformation, causes the similar vibrational mode of the carbonyl bond for PCL in the U-IC channel. Although PCL chains are in contact with each other in the amorphous phase, they are not as closely packed as in the crystalline phase.

In addition, as discussed, there are no strong interactions, such as hydrogen bonding, between included PCL and urea. This makes it possible for PCL to freely vibrate at a frequency, similar to the amorphous contribution and different from crystalline contribution, of its neat bulk sample. Thus the amorphous contribution is not indicative of the conformation or orientation of the PCL chain, but rather the packing density, which must be similar between guest PCL and Host U in the IC.

In another range of the PCL spectrum which is associated with C-O-C, it was previously[97] determined that the peak at 1187 cm^{-1} and the shoulder at 1178 cm^{-1} came from crystalline contributions while the shoulder at 1161 cm^{-1} came from the amorphous contribution. However, the overlapping of C-O-C peaks with urea peaks in this range prevent us from observing such peak shifts from that corresponding to crystalline contributions to that corresponding to the amorphous contributions. Nevertheless, interactions between PCL and urea in this region were clearly observed.

Given that excess urea was used in the procedure, the peak at 1676 cm^{-1} should be assigned

to C=O in the excess urea since it doesn't budge much from 1677 cm^{-1} for C=O in pure tetragonal urea crystal. The peak at 1653 cm^{-1} is most likely shifted from 1677 cm^{-1} which represent the C=O in tetragonal urea. This peak can be regarded as a sign of hexagonal urea channel formation. Similarly, the peak at 1463 cm^{-1} for N-C-N in tetragonal urea shifts to 1487 cm^{-1} upon formation of the hexagonal urea channel. NH_2 peaks at 1620 cm^{-1} and 1593 cm^{-1} in urea slightly shift to 1629 cm^{-1} and 1596 cm^{-1} respectively, in the PCL-U-IC. A list of the wavenumbers associated with specific bonds and groups for tetragonal urea, hexagonal urea, as-received PCL and included PCL are compared in Table 5.

Table 5 Numerical Listing of Wavenumbers at Which Some Functional Groups Absorb in the Infrared

Tetragonal Urea		Hexagonal Urea	
Peaks (cm^{-1})	Group and Class	Peaks (cm^{-1})	Group and Class
3436	NH2	3400	NH2
3341	NH2	3366	NH2
3250	NH2	3222	NH2
1677	C=O	1653	C=O
1620	NH2 or N-H	1629	NH2
1593	NH2	1596	NH2
1463	N-C-N	1487	N-C-N
Asr-PCL		PCL in the channel	
Peaks (cm^{-1})	Group and Class	Peaks (cm^{-1})	Group and Class
2944	CH2 in aliphatic	2944	CH2 in aliphatic
2865	CH2 in aliphatic	2865	CH2 in aliphatic
1723	C=O	1737	C=O
1241	C-O-C in ester	1237	C-O-C in ester
1187	C-O-C in ester	1167	C-O-C in ester

3.1.2 DSC

Despite their convenience, FTIR results are insufficient to confirm the formation of ICs. DSC was introduced in conjunction with FTIR to observe any distinguishable sign of IC formation. As seen in Figure 21, the first heating scan of PCL-U-IC does not show a melting peak for PCL. Instead, melting peaks for free U and PCL-U-IC are observed at 134 and 142° C, since excess U was employed in forming the PCL-U-IC. After melting of the PCL-U-IC, in the second heating scan we can observe melting peaks for both free PCL and U, as well as that of the partially reformed PCL-U-IC. The appearance of a PCL crystallization exotherm(~ 32 ° C) and subsequent melting endotherm(54° C) after the first heating leads us to believe that PCL was included in the PCL-U-IC crystalline structure. All four U-IC's formed using PCLs with different molecular weights were confirmed this way.

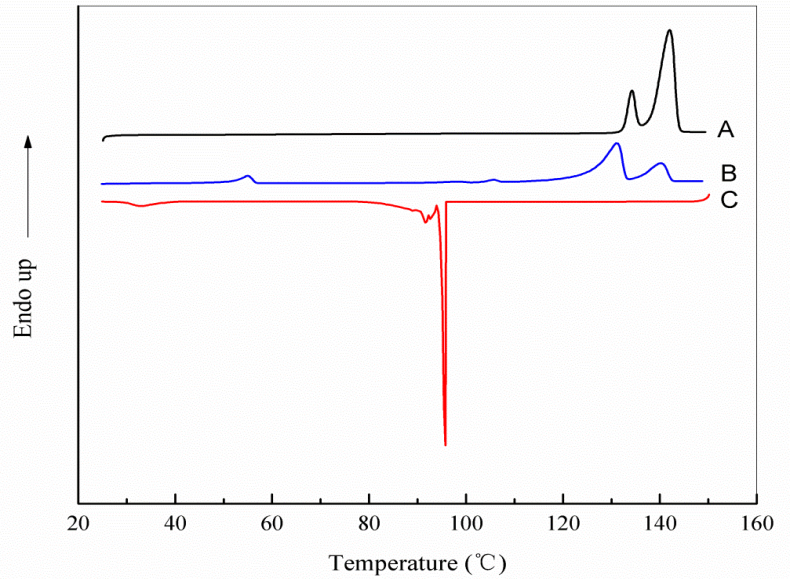

Figure 21 DSC thermograms of PCL-80-U-IC: 1st heating (A), 2nd heating (B), 1st cooling(C)

3.1.3 XRD

Powder X-ray diffraction was performed instead of single crystal diffraction, due to the difficulties associated with obtaining single crystals of PCL-U-IC. Intensity was plotted against diffraction angle, 2θ, in Figure 22, where a peak at 12.5˚ is noticeable and was previously attributed to the hexagonal structure of Polymer-U-ICs.[84] Although not shown, the tetragonal urea has very different peaks at 22.3˚, 24.6˚, 29.3˚, 31.7˚, 35.6˚ and 45.5˚. Among them, the peak at 22.3˚ has a significantly higher intensity than other peaks. However, the relative intensity of this little peak at 22.5˚ in PCL-U-IC was only 1% that of pure tetragonal urea indicating very little urea was left in the IC sample after rinsing it with methanol during the filtering process.

The most significant peak for PCL-U-IC is at 21.6˚, while semi-crystalline PCL has its strongest peak at 21.4˚, which are very close to each other. The question of whether the PCL chains were included in the U-IC matrix or retained in the bulk could be answered by performing XRD at elevated temperature above PCL and U melting temperatures. In Figure 23, PCL-U-IC was held at 130˚C, at which bulk PCLs in the sample become completely amorphous and tetragonal urea starts to melt.[83] This readily confirms that the peak at 21.6˚ was not contributed by the bulk semi-crystalline PCL.

In addition, peaks at 25˚, 27.3˚, 34.9˚, and 41.5˚, that are unique for PCL-U-IC and were not observed for both pure components, i.e., pure tetragonal urea and bulk semi-crystalline PCL, were observed. For comparison, bulk semi-crystalline PCL has three strong peaks at 21.4˚, 22˚, and 23.7˚.[99]

In summary, diffractograms in Figure 22 and 23 are essentially identical which give us another strong confirmation of PCL-U-IC formation.

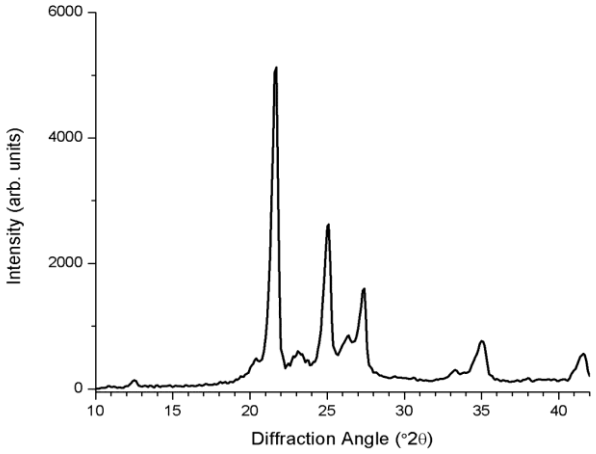

Figure 22 X-ray diffractogram of PCL-U-IC at room temperature

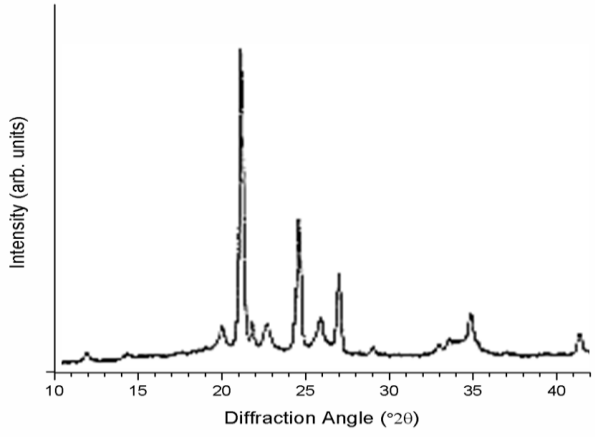

Figure 23 X-ray diffractogram of PCL-U-IC at 130˚C[83]

3.2 Confirmation of complete coalescence

3.2.1 FTIR

Coalesced PCLs were obtained from their U-ICs after removing all of the host U. As seen in the FTIR spectra presented in Figure 24, as-received and coalesced PCL are virtually identical. There is very little if any urea remaining after coalescence.

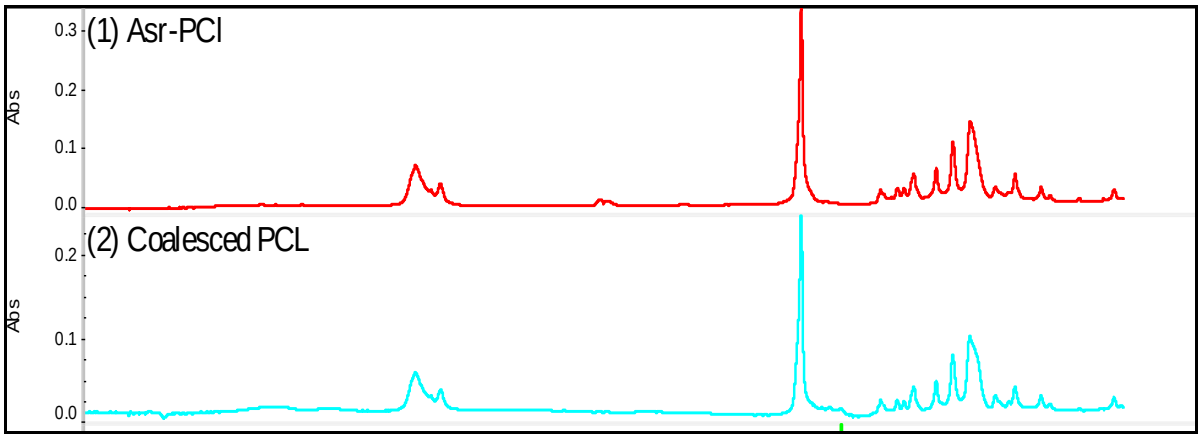

Figure 24 FTIR spectra of as-r PCL (1), c-PCL (2)

3.2.2 Proton NMR

More sensitive ^{1}H-NMR observations were also used to confirm the absence of remnant host U. (See Figure 25) The control is Asr-PCL with 10 w% of urea from which the chemical shift of urea protons and their relative intensity can be obtained. The absence of the urea proton peak at ~5.35 ppm in the spectrum of c-PCL readily confirms that there is no detectable remnant urea in our coalesced sample.

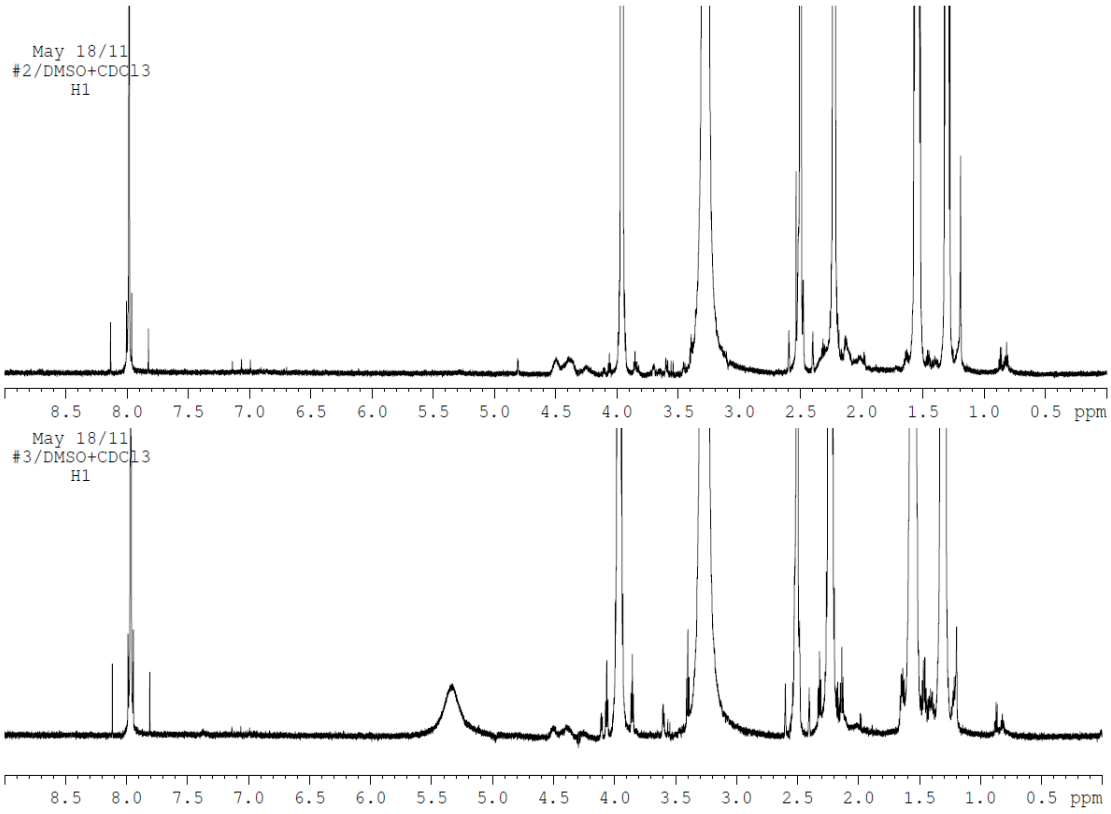

Figure 25 The 700 MHz 1H-NMR spectra of Asr-PCL with 10 w% of urea (bottom) and c-PCL (top), which have been equally expanded

3.2.3 Flow time

Flow times for as-received and coalesced PCL 80,000 of equal concentration of 0.5g/dL in acetone were measured in a #50 Cannon-Ubbelohde viscometer at room temperature. (See Table 6) The flow times of both solutions are very similar, which reassures us that there is no degradation occurring during the IC formation and coalescence processes. In addition, similar flow times indicate that there is no appreciable urea content in our coalesced PCL, since any insoluble impurities in both solutions have been filtered to prevent it from clogging

the viscometer capillary.

Table 6 Flow time of asr-PCL and c-PCL

Sample	Flow time*
Acetone	**86 seconds**
asr-PCL	**122 seconds**
c-PCL	**124 seconds**

**average over 3 readings*

3.3 Thermal Properties[100]

3.3.1 Melt-crystallization properties

The melt-crystallization of as-received (asr-) and c-PCL samples were studied by DSC. It is clear from Table 7 and Figure 26 that all c-PCL melts crystallize at significantly higher temperatures than their corresponding asr-melts, with the difference between them increasing with their molecular weights. It is also apparent that the T_c of the highest molecular weight asr-sample (PCL-80) is significantly lower than the T_cs of the others, which are very similar. This may be due to the presumably highly entangled nature of the high molecular weight asr-PCL-80 melt.

Despite the vast differences in their molecular weights, all the c-PCL samples have similar melt-crystallization temperatures. This is consistent with the assumed extended, un-entangled natures of their constituent PCL chains. (See Figure 7)

Table 7 Crystallization temperatures of different molecular weight asr- and c-PCLs

Sample	T_c of asr-PCLs, °C	T_c of c-PCLs, °C
PCL-2	**17.0**	**26.5**
PCL-10	**16.8**	**32.5**
PCL-40	**18.8**	**35.0**
PCL-80	**11.7**	**33.3**

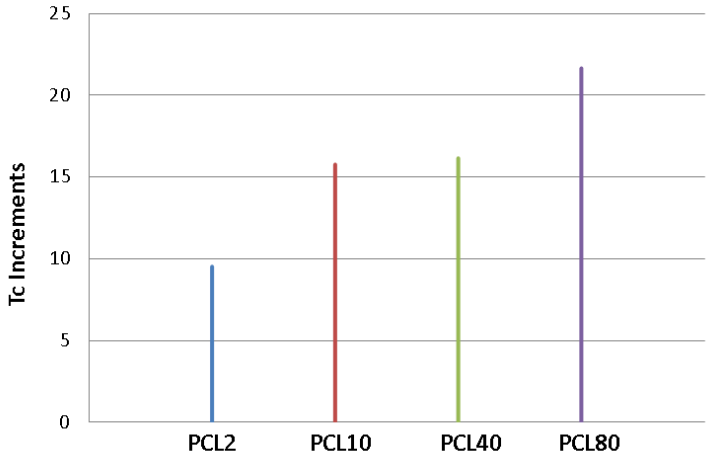

Figure 26 Tc increments = Tc (c-PCL) - Tc (asr-PCL) for PCL-2, -10, -40, and -80

3.3.2 Prolonged annealing

The distinction between the T_cs of asr- and c-PCLs is maintained even after prolonged melt annealing of their c-melts at 80º C, as can be seen in Table 8. The difference in molecular

weights, no matter whether above or below the molecular weight of entanglement (Me), does not interfere with their thermal stabilities. This behavior suggested that c-PCLs would make excellent nucleation agents for enhancing the melt-crystallization of asr-PCLs.

Table 8 Crystallization temperatures of c-PCLs before and after annealing 2 and 4 weeks at 80° C

Sample	Initial T_c (°C)	T_c (°C) after annealing 2 weeks at 80° C	T_c (°C) after annealing 4 weeks at 80° C
c-PCL-2	**26.5**	**26.0**	**26.4**
c-PCL-10	**32.5**	**30.9**	**31.7**
c-PCL-40	**35.0**	**34.1**	**33.8**
c-PCL-80	**33.3**	**30.1**	**31.1**

3.3.3 Self-Nucleation effect

One of the applications of our coalesced PCLs is to act as "stealth" nucleating agents to improve the melt-crystallization of asr-PCLs. The evaluation of the nucleating effect was carried out by DSC. In Figure 27 the first cooling DSC scans of neat asr-PCL-40, c-PCL-40, and asr-PCL-40 (97.5 wt%) self-nucleated with c-PCL-40 (2.5 wt%) reveal that the resulting nuc-PCL-40 and neat c-PCL-40 crystallize more readily than asr-PCL-40. The crystallization exotherms of c- and nuc-PCL-40 are much narrower/sharper, with crystallization ranges of ~

9-10° C compared with ~30 °C for asr-PCL-40, and occur at significantly higher temperatures (35 and 32.3º C, respectively) compared with the crystallization exotherm of asr-PCL-40 (18.8º C).

Table 9 presents a comparison of melt-crystalization temperatures for asr- , c-, and nuc- samples of all four PCLs. In addition to the self-nucleated samples, the T_cs of asr-PCL-2, -40, -80 nucleated with c-PCL-10 are also given there, and they are seen to differ only minimally from the T_cs of their self-nucleated films. We can also see that the crystallization of nuc-PCL-2 is very similar to and not enhanced compared with asr-PCL-2, independent of whether it is self-nucleated or nucleated with c-PCL-10. This is likely a result of its very low molecular weight, corresponding to just 16 repeat units (See Table 4), but not to the absence of entanglements, because all of the c-PCL melts are believed to crystallize from un-entangled melts. C-PCL-2 crystallizes less than 10° C higher than asr-PCL-2, while the higher molecular weight c-PCLs crystallize from 16 to 22° C higher in temperature than their asr-samples. The -20° C/min cooling rate employed may not allow time sufficient for the asr-PCL chains to fully crystallize even though the nucleating c-PCL chains already have. Crystallinities calculated from 2nd heating DSC scans, assuming ΔH_m^o = 135 J/g, are as follows: asr-, c-, and nuc-PCL80s are ~ 34±2% crystalline. If they have been melt pressed into film and are held at RT for a long time, all their crystallinities increase to ~ 50%. PCL40: asr- and nuc- ~ 49% crystallinities, PCL10: asr- and nuc- ~ 47% crystallinities, and PCL2: asr- and nuc- have ~60% crystallinities.

Table 9 Crystallization temperatures, Tc, of different molecular weight as-received PCLs, self-nucleated PCLs, and PCLs nucleated with c-PCL-10

Sample	T_c, ° C			
	PCL-2	PCL-10	PCL-40	PCL-80
As-received	17.0	16.8	18.8	11.7
Coalesced	26.5	32.5	35	33.3
Self-nucleated	18.8	27.9	32.3	29.6
Nucleated with c-PLC-10	21.3	27.9	29.5	28.1

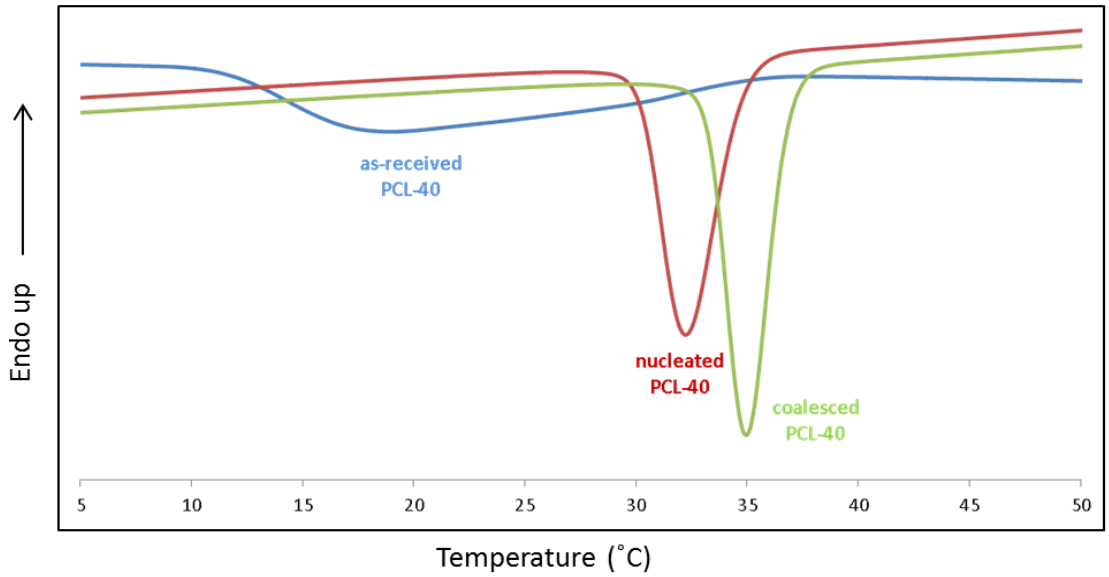

Figure 27 First cooling DSC scans from the melts of neat asr-PCL-40, self-nucleated nuc-PCL-40 (2.5 wt% c-PCL-40 + 97.5 wt% asr-PCL-40), and coalesced PCL-40

3.3.4 Semi-Crystalline Morphology

In Figure 28, the optical microscope images of asr- and c-PCL-10 and -40 films observed under crossed polarizers are presented. There it is clear that the c-PCL-10 and -40 films have finer scale, more homogeneous semi-crystalline morphologies compared to their asr-received films. However, differences between different molecular weight samples are also evident. The nucleation rate is more dependent on the molecular weight than spherulite growth rate is. That is to say, the increase of nucleation rate is faster than the increase of growth rate with the increase in molecular weight. This will result in a higher nucleation density and smaller crystals for the higher molecular weight samples. In the light of this, only in lower molecular weight samples can we clearly see single spherulites and the differences between their relative sizes for asr- and c-PCLs.

3.3.5 Section Summary

All four PCLs, with molecular weights ranging from well below to well above the reported entanglement molecular weight of PCL, ~15,000 g/mol, when coalesced from their U-ICs are reorganized in a manner that significantly increases their melt-crystallization temperatures above those of their asr-samples. The difference in their thermal behaviors, and presumably their structures, is retained in their melts for extensive periods of time (See Table 8). Those behaviors presumably result from the small un-oriented regions of extended and un-entangled chains with no overall macroscopic orientation of the small regions of extended and un-entangled chains.[100]

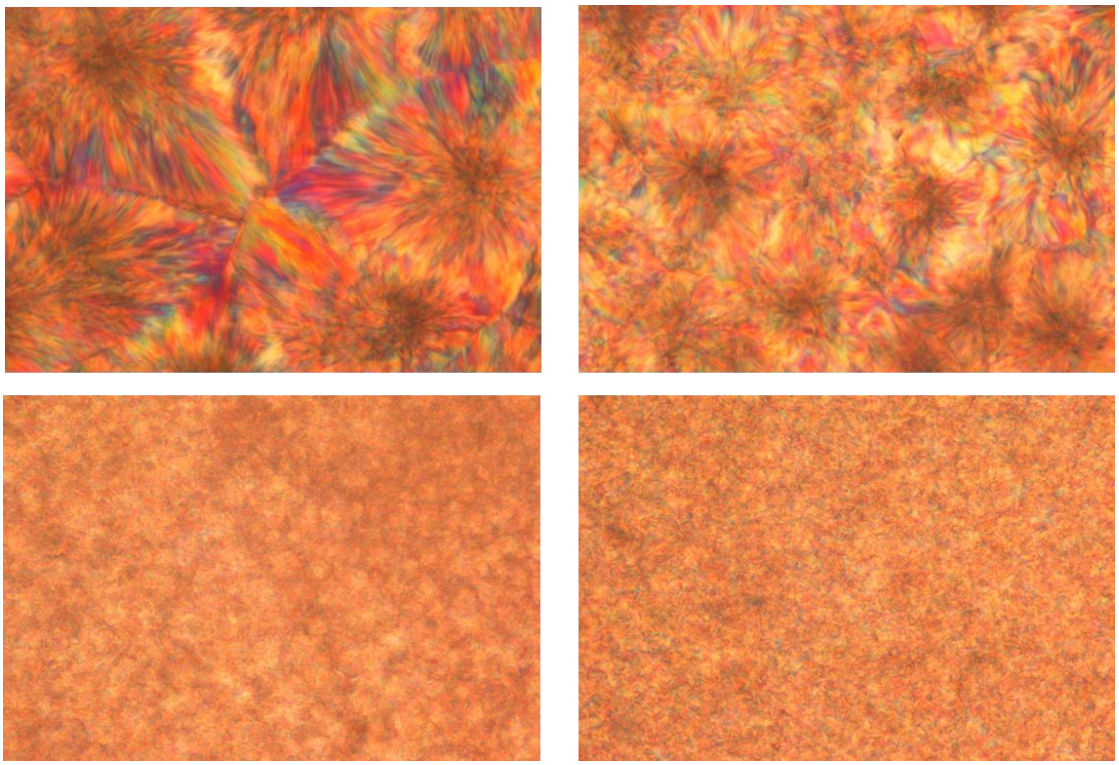

Figure 28 Optical microscopy images (500x, crossed polarizers, ¼ λ plate) of melt pressed asr-PCL-10 (top left), c-PCL-10 (top right), asr-PCL-40(bottom left) and c-PCL-40(bottom right) films

3.4 Physical properties

3.4.1 Density

The unique and improved melt crystallization behaviors of coalesced PCL were believed to be the result of small un-oriented regions of extended chains without overall macroscopic orientation. It is reasonable to expect the change in conformation of polymer chains would be reflected in the overall density of the bulk material.

Melt pressed films of both asr-PCL and c-PCL were made using the same process condition. The density of each sample was averaged over four measurement and was determined to be 1.144 and 1.146 g/cm^3 for as-received and coalesced PCL respectively.(See Table 10) Multiple independent measurements made on different days showed slight shifts in both values with their differences remaining constant at ca. 0.2%. DSC results show essentially equal crystallinity for both samples, leading to the calculated increase in amorphous region density of c-PCL of ca. 0.4%. This indicates a tighter packing of coalesced polymer chains in the amorphous phase compared to the randomly coiling as-received polymer chains. Additional measurements were performed to compare the density of c-PCLs from U- and from CD-ICs, which the latter c-PCL showed ~0.6% higher density. The FTIR spectrum of c-PCL from CD confirmed complete removal of CD. The reason for such a large difference between coalesced PCLs from inclusion compounds made with different hosts (CDs and U) remains unknown.

Table 10 Densities of asr-PCL and c-PCL

Sample	**Density***
asr-PCL	**1.144 g/cm^3**
c-PCL	**1.146 g/cm^3**
Overall Increase	**0.2%**
Amorphous Increase	**0.4%**

Average over 4 readings

3.4.2 Nano-indentation

Nano-indentation provides us with nano to micro scale surface mechanical properties of a thin film. This is an especially valuable technique for investigating hardness and Young's modulus of low yield materials. Williamson et al.[5] introduced Nano-indentation to test PCL coalesced from α-CD, since the tedious coalescence process deterred them from accomplishing tensile tests which demands much more coalesced material. Nano-indentation was carried out here for the purpose of comparing the hardness and Young's modulus between c-PCL from α-CD and Urea ICs.

Hardness and Reduced modulus were automatically calculated by the software using the means introduced in the previous chapter. Some obvious statistical outliers were removed from the data set. Young's modulus was calculated using the Young's modulus of diamond indenter, and Poisson's ratios for both diamond and PCL.

Average hardness for both the as-received and coalesced PCL films as a function of testing stress are plotted in Figure 29. Vertical error bars indicate the standard error of the estimated mean of the hardness. In order to compare the hardness of c-PCL films from U and CD, the value for as-received sample should be examined first. Hardness of as-received PCL film in the current test ranged from 0.029 to 0.039 GPa, which is in close approximation with the value from the previous work (~0.033-0.037 GPa).[5] With confidence in the value of as-received PCL, hardness for c-PCL films from U and CD can be compared. Close examination revealed that the value for c-PCL from U-IC at the lowest stress (500μN) was extremely high, and probably due to the deviation of actual contact area from the area

function and to the different near surface properties. Comparing the data at 1000, 1500 and 2000 μN confirmed that the hardness of c-PCL from U (~0.043-0.057 GPa) is essentially similar to that of c-PCL from α-CD. (~0.043-0.051GPa)

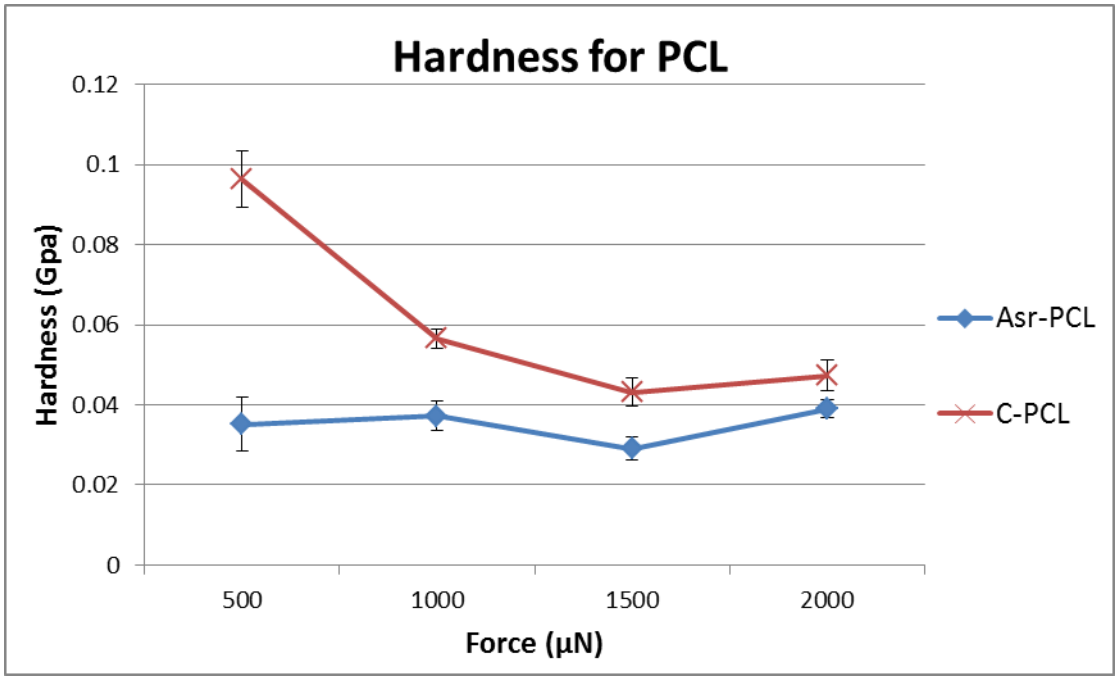

Figure 29 Hardness as a function of testing stress for as-received and coalesced from U-IC PCLs

The average Young's modulus as a function of testing stress is plotted in Figure 30. Vertical error bars indicate the standard error for the estimated mean of Young's modulus. Still a depth related trend was observed from the decrease in the Young's modulus of the material with the increase in testing stress. Plotting modulus against depth was previously used to account for the substrate effect for extremely thin film.[101] In our case, the maximum depth for

2000μN is ~3000nm, only ~1% of total thickness of the film. Instead of observing substrate effect, the deeper the indentation, the more characteristic of bulk material the result is.

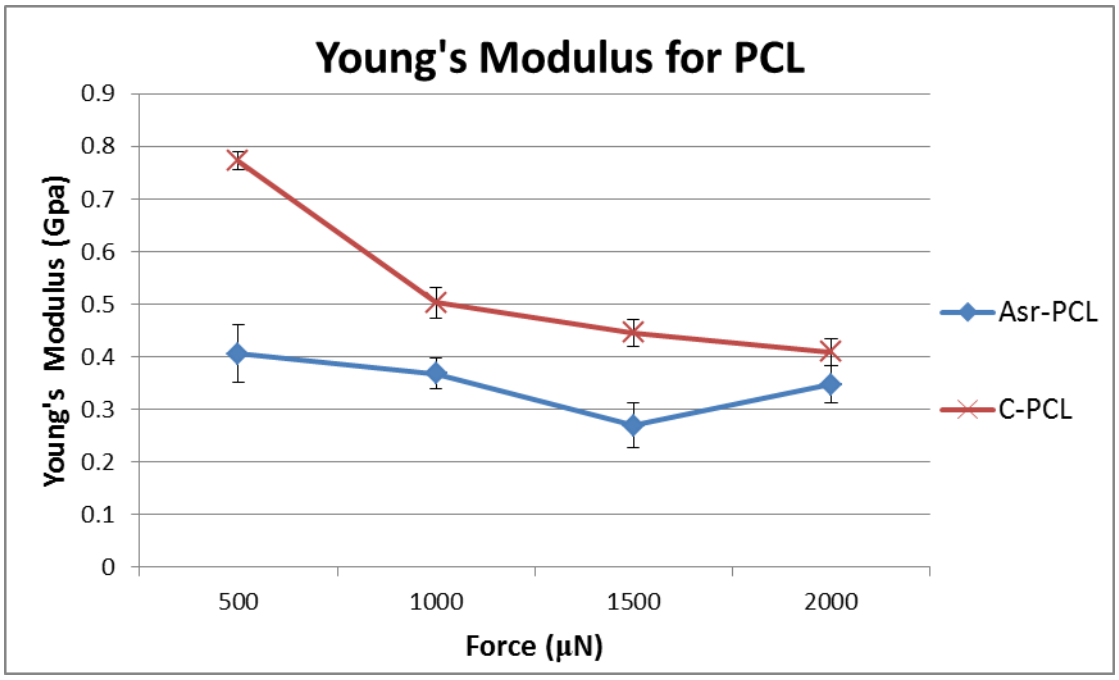

Figure 30 Young's modulus as a function of testing stress for as-received and coalesced from U-IC PCLs

Young's modulus for both asr- and c-PCL were plotted against maximum depth in Figure 31. A power function was automatically fitted by Excel software and was determined to be better than a quadratic polynomial between the data range of 500-3000 nm. In order to better estimate bulk properties of the films, maximum depths were set as 3000nm (the upper limit of the fitted function) for both asr- and c-PCL power function. Therefore, Young's modulus

of 0.1526 and 0.2241 GPa were obtained from the fitted function at 3000nm. Here we suspect that these results give us a better approximation to the bulk properties of PCLs.

However, there are a few reasons for further performing standard tensile test. First of all, the indentation area is so small that is susceptible to any defect, such as air bubbles, dirt and grains on the die. Second, the indentation measures recovery after compression as opposed to elongation under tension in tensile testing.

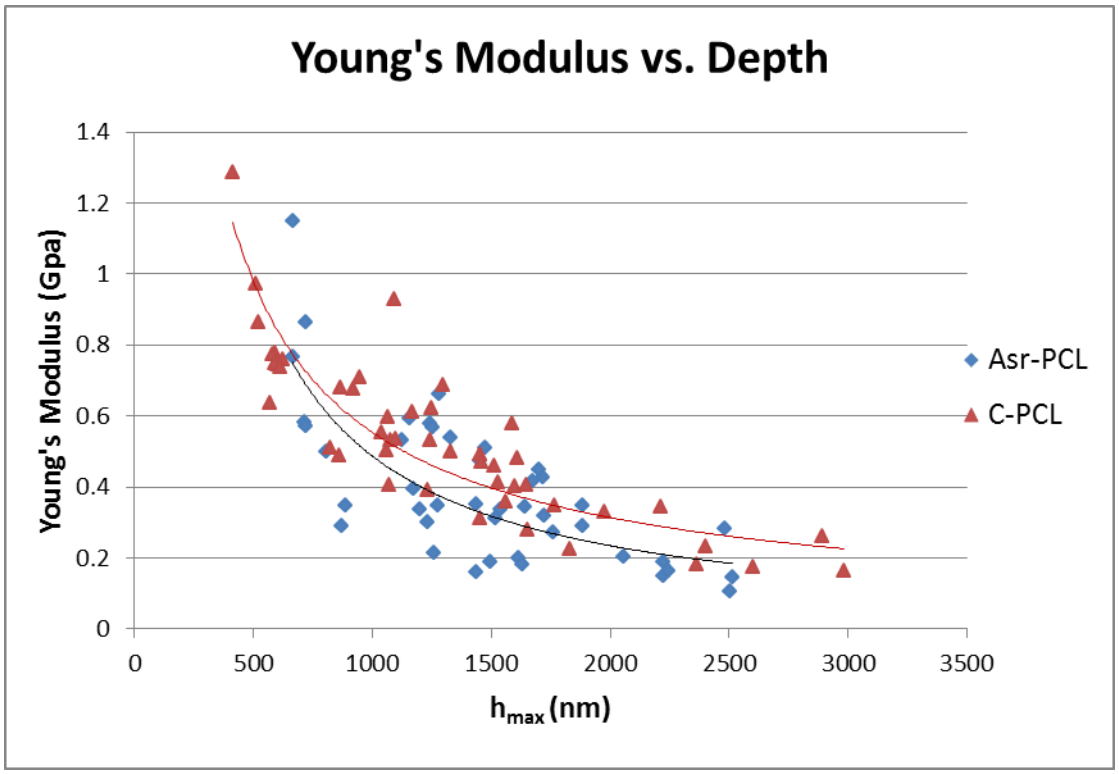

Figure 31 Young's modulus as a function of maximum depth for as-received and coalesced from U-IC PCLs

3.4.3 Tensile Tests

Tensile tests were performed on ~0.3-0.4 mm thick melt pressed films trimmed with a standard template. The average value for properties of interest and their standard deviations are listed in Table 11. Typical load-elongation curves are plotted in Figure 32 for both as-received and coalesced PCL. From there we can see c-PCL has a higher Young's modulus and yield load, but has lower elongation at break compared to asr-PCL. It is worth mentioning here that a parallel study on c-PCL from CDs showed much lower elongation at break and therefore showed very low toughness. On the other hand, this brittle behavior was overcome by c-PCL from U, as evidenced by the essentially similar overall areas under the curve (toughness) compared to asr-PCL.

Table 11 Mechanical properties of asr-PCL and c- PCL

Properties	As-r	Coalesced	%Change
Strain% at Break	891.0±33.4%	841.2±72.9%	-5.6%
Modulus (MPa)	158.6±8.0	210.5±10.7	32.7%
Yield stress (MPa)	10.9±1.0	11.60±0.9	6.4%
Energy to break (Nmm)	19600±2000	19800±4200	0.8%

Close scrutiny of other mean values and standard deviations revealed that all of these differences, except Modulus, have overlapping standard deviations and therefore they do not significantly differ from each other. Modulus, however, has a much higher and significant increase (~33%) from asr-PCL to c-PCL. (See Figure 33)

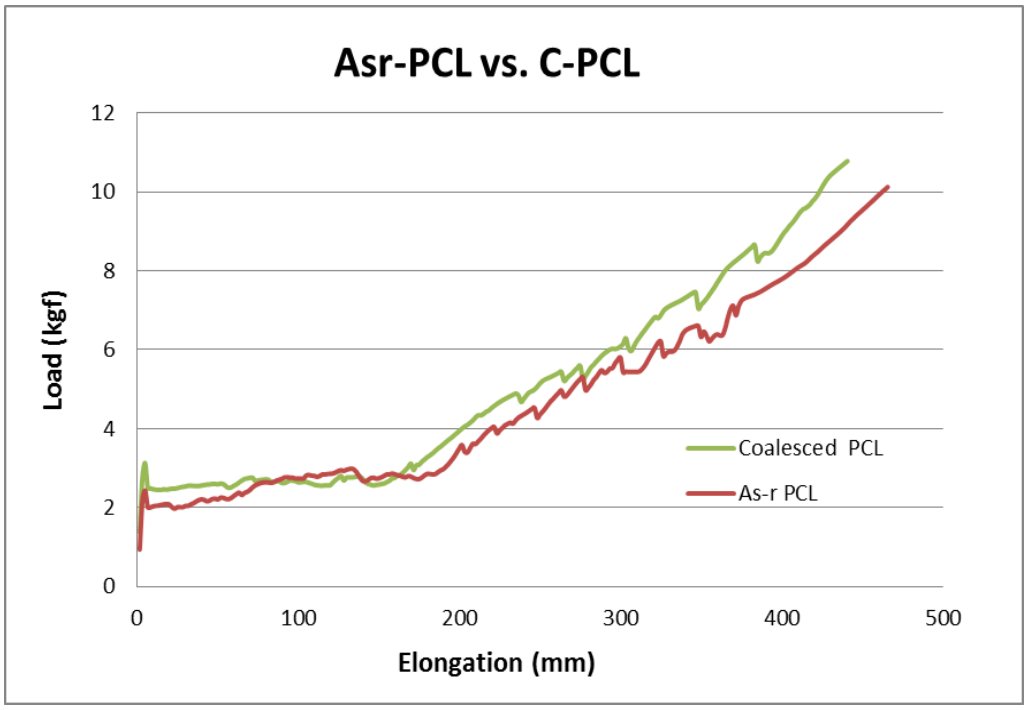

Figure 32 Load-Elongation curves for as-received and coalesced PCL

Although tested by different means, it would be interesting to compare Young's modulus obtained in tensile tests to those from Nano-indentation. From Figure 30 we can see that the average Young's modulus obtained by Nano-indentation is much higher than what we obtained in the tensile tests. Because of the depth related trend, it is not legitimate to use mean value averaging over all testing forces to characterize the bulk property of PCL.

However, when the depth is set to the largest reliable value for the fitted function (3000nm), moduli from Nano-indentation are similar to tensile test results. The modulus obtained after the inclusion and coalescence process increases from 158.6 to 210.5 MPa in tensile tests, and from 152.5 to 224.1 MPa in Nano-indentation. That both methods show significant improvement of modulus from as-received PCL to coalesced PCL confirm the expectation of properties resulting from extended un-entangled chains that are packed together more closely in the non-crystalline sample regions. (See Figure 12)

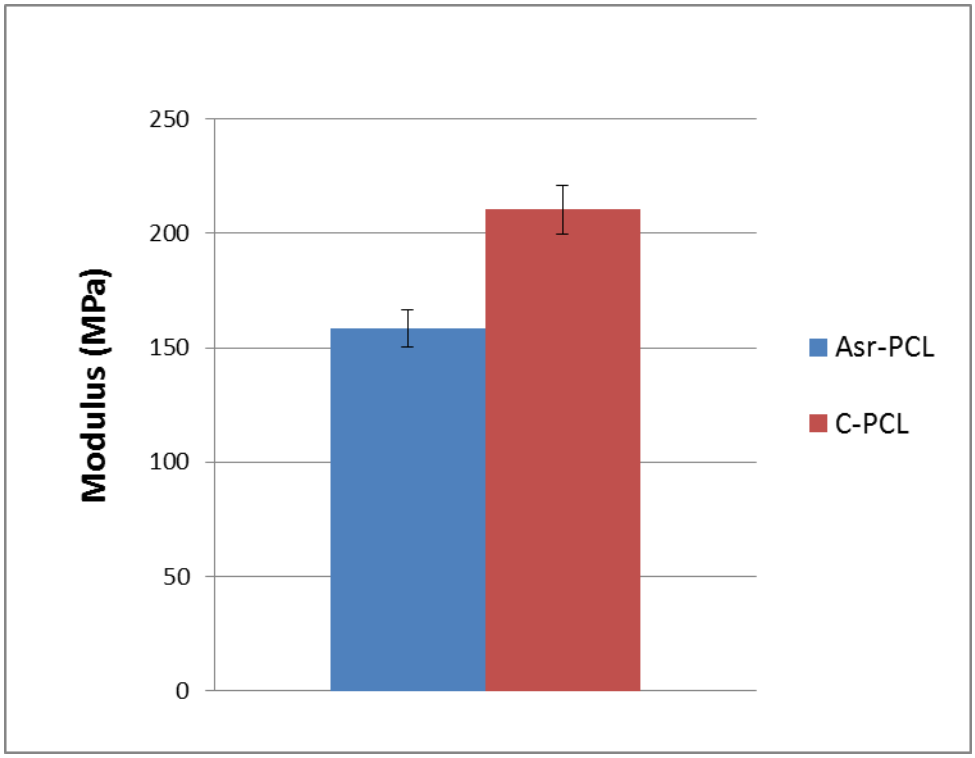

Figure 33 Modulus increment from asr- to c-PCL from tensile tests

Chapter 4: Conclusions

PCLs coalesced from their U-ICs show enhanced abilities to crystallize, regardless of their molecular weight, over samples processed normally from their melts and solutions. This is consistent with PCL and other polymer guests coalesced from their ICs formed with host CDs. The retention of the enhanced abilities of PCLs coalesced from their U-ICs to crystallize even after spending long times (weeks or more) in the melt was also similar to its analog obtained from PCL-α-CD-IC. However, unlike CD hosts, U does not thread over guest polymer chains when forming their ICs. This makes it possible to conclude that the enhanced ability of c-PCLs to crystallize from their melts upon removal of the host U molecules is solely a consequence of their coalesced conformations, structures, and morphologies, which are stable to prolonged melt-annealing.

Since both coalesced PCLs behave similarly, it is reasonable to exclude the effect of remnant CD host when accounting for their enhanced performance. Furthermore, because c-PCLs with chain lengths well below and well above those corresponding to the entanglement molecular weight of PCL behave similarly, we conclude that their enhanced ability to crystallize from the melt is likely a consequence of the extended and un-entangled arrangement of their coalesced chains.

The high productivity of coalesced PCL obtained from Urea compared to that from CD makes it possible to have enough material for various physical tests. The viscometer flow times for both asr-PCL and c-PCL confirmed that there was no degradation during the IC

formation and coalescence processes. Density measurement showed an increase of ca. 0.2% and 0.4% for overall and amorphous region densities respectively. Nano-indentation results showed enhanced hardness and Young's modulus of c-PCL over asr-PCL, with the calculated values decreasing with an increase in indentation depth. Maximizing the indentation depth in the fitted power function with the upper limit of data available led to moduli approaching those observed in bulk tensile tests. Tensile testing showed a slight increase in yield stress and decrease in the elongation of c-PCL, with only the increase in modulus being statistically significant. In addition to the direct use of c-PCL, small amounts of c-PCL can also be used as a fully compatible "stealth" nucleant for the melt-processing of asr-PCL.

In conclusion, with the improvement made to PCL by nano-processing with U or CDs, the use of PCL in load-bearing bio-medical applications can be effectively enlarged.

Chapter 5: Future Directions

The behaviors observed for c-PCL are consistent with the anticipated extended and un-entangled conformations of the coalesced polymer melt. Though challenging, it would be worth directly observing the apparently unique structure and organization of coalesced polymers in their melts. Because polymer melts are usually featureless when observed by microscopy, AFM and POM equipped with hot stages might be a possible choice to investigate the kinetics of crystallization behavior in the vicinity of nucleation. Useful information might be obtained from such real-time imaging of the crystallization process.

The enhancement observed for various physical properties gives us the confidence in believing that other properties specifically important for certain applications are also changed, *e.g.*, moisture and gas permeability. The superior c-PCL films can also be used as self-reinforcement in single component composites.[88] Since self-nucleation was determined to be effective, it is worthwhile to see if repeated self-nucleation with nucleated PCL works or not. In addition, as previously done by forming common ICs with CD, inherently immiscible polymer pairs could also possibly be mixed at the molecular level by forming common ICs with host urea.[12, 102-109]

References

(1) Brandrup, J.; Immergut, E. H.; Grulke, E. A.; Abe, A.; Bloch, D. R. Polymer Handbook (4th Edition).

(2) Tonelli, A. E. In *Polymers From the Inside Out: An Introduction to Macromolecules;* Wiley-Interscience: New York, 2001; , pp 249.

(3) Gross, R. A.; Kalra, B. Biodegradable Polymers for the Environment. *Science* **2002**, *297*, 803-807.

(4) Labet, M.; Thielemans, W. Synthesis of polycaprolactone: a review. - *Chem. Soc. Rev.* **2009**, *38*, 3484-3504.

(5) Williamson, B. R.; Krishnaswamy, R.; Tonelli, A. E. Physical properties of poly(ε-caprolactone) coalesced from its α-cyclodextrin inclusion compound. *Polymer* **2011**, *52*, 4517-4527.

(6) Dash, T. K.; Konkimalla, V. B. Poly-ϵ-caprolactone based formulations for drug delivery and tissue engineering: A review. *J. Controlled Release* **2011**, *xxx*, xxx-xxx.

(7) Joshi, P.; Madras, G. Degradation of polycaprolactone in supercritical fluids. *Polym. Degrad. Stab.* **2008**, *93*, 1901-1908.

(8) Sivalingam, G.; Karthik, R.; Madras, G. Kinetics of thermal degradation of poly(ε-caprolactone). *J. Anal. Appl. Pyrolysis* **2003**, *70*, 631-647.

(9) Odian, G. In *Step Polymerization;* Principles of Polymerization; John Wiley & Sons, Inc.: 2004; 2004; pp 39-197.

(10) Odian, G. In *Chain Copolymerization;* Principles of Polymerization; John Wiley & Sons, Inc.: 2004; 2004; pp 464-543.

(11) Rohindra, D. R.; Khurma, J. R. Miscibility, melting and crystallization of poly(ε-caprolactone) and poly (vinyl formal) blend. *S. Pac. J. Nat. App. Sci.* **2007**, *25*, 53-60.

(12) Rusa, C. C.; Tonelli, A. E. Polymer/polymer inclusion compounds as a novel approach to obtaining a PLLA/PCL intimately compatible blend. *Macromolecules* **2000**, *33*, 5321-5324.

(13) Qiu, Z.; Komura, M.; Ikehara, T.; Nishi, T. Miscibility and crystallization behavior of biodegradable blends of two aliphatic polyesters. Poly(butylene succinate) and Poly(ε-caprolactone). *Polymer* **2003**, *44*, 7749-7756.

(14) Castillo, R. V.; MuÌˆller, A. J.; Raquez, J.; Dubois, P. Crystallization Kinetics and Morphology of Biodegradable Double Crystalline PLLA-b-PCL Diblock Copolymers. *Macromolecules* **2010**, *43*, 4149-4160.

(15) Vanneste, M.; Groeninckx, G.; Reynaers, H. Miscibility, crystallization and melting behaviour and semicrystalline morphology of ternary blends of poly(ε-caprolacton), poly(hydroxy ether of bisphenol A) and poly(styrene-co-acrylonitrile): 2. Semicrystalline morphology. *Polymer* **1997**, *38*, 4407-4411.

(16) Di Maio, E.; Iannace, S.; Sorrentino, L.; Nicolais, L. Isothermal crystallization in PCL/clay nanocomposites investigated with thermal and rheometric methods. *Polymer* **2004**, *45*, 8893-8900.

(17) Eastmond, G. Poly(ε-caprolactone) Blends. *Adv Polym Sci* **1999**, *149*, 59-223.

(18) Phillips, P. J.; Rensch, G. J.; Taylor, K. D. Crystallization studies of poly(ε-caprolactone).I. Morphology and kinetics. *Journal of Polymer Science Part B: Polymer Physics* **1987**, *25*, 1725-1740.

(19) Chen, H.; Li, L.; Ou-Yang, W.; Hwang, J. C.; Wong, W. Spherulitic Crystallization Behavior of Poly(ε-caprolactone) with a Wide Range of Molecular Weight. *Macromolecules* **1997**, *30*, 1718-1722.

(20) Dhanvijay, P. U.; Shertukde, V. V.; Kalkar, A. K. Isothermal and nonisothermal crystallization kinetics of poly(ε-caprolactone). *J Appl Polym Sci* **2012**, *124*, 1333-1343.

(21) Zhuravlev, E.; Schmelzer, J. W. P.; Wunderlich, B.; Schick, C. Kinetics of nucleation and crystallization in poly(ε-caprolactone) (PCL). *Polymer* **2011**, *52*, 1983-1997.

(22) Acierno, S.; Di Maio, E.; Iannace, S.; Grizzuti, N. Structure development during crystallization of polycaprolactone. *Rheologica Acta* **2006**, *45*, 387-392.

(23) Albertsson, A.; Varma, I. Aliphatic Polyesters: Synthesis, Properties and Applications. *Adv Polym Sci* **2002**, *157*, 1-40.

(24) Edlund, U.; Albertsson, A. Degradable Polymer Microspheres for Controlled Drug Delivery. *Adv Polym Sci* **2002**, *157*, 67-112.

(25) Sinha, V. R. Poly-ϵ-caprolactone microspheres and nanospheres: an overview. *Int. J. Pharm.* **2004**, *278*, 1-23.

(26) Flory, P. J. In *Principles of Polymer Chemistry;* Cornell University Press: Ithaca, New York, 1953; , pp 688.

(27) Tonelli, A. E. Conformations and motions of polyethylene and poly(oxyethylene) chains confined to channels. *Macromolecules* **1990**, *23*, 3134-7.

(28) TONELLI, A. Modeling the Conformations and Mobilities of Aliphatic Polyamides and Polyesters Confined to Channels. *Macromolecules* **1991**, *24*, 1275-1278.

(29) TONELLI, A. Conformations and Motions of Polypropylenes Confined to Channels. *Macromolecules* **1991**, *24*, 3069-3073.

(30) Tonelli, A. E. Polylactides in channels. *Macromolecules* **1992**, *25*, 3581-4.

(31) Tonelli, A. E. Can polymers containing rings in their backbones form inclusion compounds with small-molecule, host clathrates? *Comput. Polym. Sci.* **1992**, *2*, 80-83.

(32) Tonelli, A. E. Modeling the conformations and motions of isolated polymer chains in the narrow channels of their crystalline inclusion compounds with small-molecule, host clathrates. *Polym. Prepr. (Am. Chem. Soc. , Div. Polym. Chem.)* **1992**, *33*, 551-2.

(33) TONELLI, A. Polylactides in Channels. *Macromolecules* **1992**, *25*, 3581-3584.

(34) HOWE, C.; SANKAR, S.; TONELLI, A. C-13 Nmr Observation of Poly(l-Lactide) in the Narrow Channels of its Inclusion Compound with Urea. *Polymer* **1993**, *34*, 2674-2676.

(35) VASANTHAN, N.; SHIN, I.; TONELLI, A. Conformational and Motional Characterization of Isolated Poly(epsilon-Caprolactone) Chains in their Inclusion Compound Formed with Urea. *Macromolecules* **1994**, *27*, 6515-6519.

(36) Shin, I.; Vasanthan, N.; Nojima, S.; Tonelli, A. NMR relaxation observations of the constrained segmental motions of block copolymers in the narrow channels of their inclusion compound crystals formed with urea. *Abstr. Pap. Am. Chem. Soc.* **1997**, *213*, 547-POLY.

(37) Shin, I.; Huang, L.; Tonelli, A. NMR observation of the conformations and motions of polymers confined to the narrow channels of their inclusion compounds. *Macromol. Symp.* **1999**, *138*, 21-40.

(38) Rusa, C.; Luca, C.; Tonelli, A.; Rusa, M. Structural investigations of the poly(epsilon-caprolactam)-urea inclusion compound. *Polymer* **2002**, *43*, 3969-3972.

(39) Lu, J.; Mirau, P. A.; Tonelli, A. E. Chain conformations and dynamics of crystalline polymers as observed in their inclusion compounds by solid-state NMR. *Prog. Polym. Sci.* **2002**, *27*, 357-401.

(40) Huang, L.; Gerber, M.; Taylor, H.; Lu, J.; Tapaszi, E.; Wutkowski, M.; Hill, M.; Lewis, C.; Harvey, A.; Herndon, A.; Wei, M.; Rusa, C.; Tonelli, A. Creation of novel polymer materials by processing with inclusion compounds. *Macromol. Symp.* **2001**, *176*, 129-144.

(41) Shuai, X.; Wei, M.; Porbeni, F.; Bullions, T.; Tonelli, A. Formation of and coalescence from the inclusion complex of a biodegradable block copolymer and alpha-cyclodextrin.

2: A novel way to regulate the biodegradation behavior of biodegradable block copolymers RID C-5819-2008. *Biomacromolecules* **2002**, *3*, 201-207.

(42) Tonelli, A.; Rusa, C.; Bullions, T.; Wei, M.; Shuai, X. Reorganization of polymers by processing with their cyclodextrin inclusion compounds. *Abstr. Pap. Am. Chem. Soc.* **2003**, *225*, U638-U638.

(43) Tonelli, A.; Bullions, T.; Wei, M.; Wang, X.; Uyar, T. Nanostructuring polymer conformations to alter their properties. *Abstr. Pap. Am. Chem. Soc.* **2003**, *226*, U409-U409.

(44) Tonelli, A. Reorganization of the structures, morphologies, and conformations of polymers by coalescence from their crystalline inclusion compounds formed with cyclodextrins. *Macromol. Symp.* **2003**, *203*, 71-87.

(45) Rusa, M.; Uyar, T.; Busche, B.; Tonelli, A. Nanostructuring polymers with cyclodextrins - Adjusting their conformations and organizing polymers on surfaces. *Abstr. Pap. Am. Chem. Soc.* **2004**, *228*, U509-U509.

(46) Rusa, C.; Wei, M.; Bullions, T.; Rusa, M.; Gomez, M.; Porbeni, F.; Wang, X.; Shin, I.; Balik, C.; White, J.; Tonelli, A. Controlling the polymorphic behaviors of semicrystalline polymers with cyclodextrins RID A-5886-2010. *Cryst. Growth Des.* **2004**, *4*, 1431-1441.

(47) Rusa, C.; Shuai, X.; Shin, I.; Bullions, T.; Wei, M.; Porbeni, F.; Lu, J.; Huang, L.; Fox, J.; Tonelli, A. Controlling the behaviors of biodegradable/bioabsorbable polymers with cyclodextrins RID C-5819-2008. *J. Polym. Environ.* **2004**, *12*, 157-163.

(48) Uyar, T.; Rusa, C.; Hunt, M.; Aslan, E.; Hacaloglu, J.; Tonelli, A. Reorganization and improvement of bulk polymers by processing with their cyclodextrin inclusion compounds. *Polymer* **2005**, *46*, 4762-4775.

(49) Hunt, M. A.; Busche, B. J.; Rusa, M.; Uyar, T.; Rusa, C. C.; Balik, C. M.; Tonelli, A. E. Controlling the nanostructure of polymers with cyclodextrins RID A-5886-2010. *Abstr. Pap. Am. Chem. Soc.* **2006**, *231*.

(50) Tonelli, A. E. Nanostructuring and functionalizing polymers with cyclodextrins. *Polymer* **2008**, *49*, 1725-1736.

(51) Atwood, J. L. In *Inclusion Compounds;* Ullmann's Encyclopedia of Industrial Chemistry; Wiley-VCH Verlag GmbH & Co. KGaA: 2000; .

(52) Harris, K. D. M.; - Thomas, J. M. Structural aspects of urea inclusion compounds and their investigation by X-ray diffraction: a general discussion. *J. Chem. Soc. , Faraday Trans.* **1990**, *86*, 2985-2996.

(53) TONELLI, A. Modeling the Conformations and Motions of Isolated Polymer-Chains in the Narrow Channels of their Crystalline Inclusion-Compounds with Small-Molecule, Host Clathrates. *Abstr. Pap. Am. Chem. Soc.* **1992**, *203*, 221-POLY.

(54) Anonymous Clathrate compound. *http://en.wikipedia.org/wiki/Clathrate* (accessed 3/5, 2012).

(55) Villiers, A. Sur la transformation de la fécule en dextrine par le ferment butyrique. *Compt. Rend. Fr. Acad. Sci.* **1891**, *112*, 536-538.

(56) Schardinger, F. Über thermophile bakterien aus verschiedenen Speisen und milch, sowie über einige Umsetzungsprodukte derselben in kohlenhydrathaltigen Nährlösungen, darunter krystallisierte polysaccharide (dextrine) aus stärke. *Z. Untersuch. Nahr. u. Genussm.* **1903**, *6*, 865-880.

(57) Schardinger, F. Bildung kristallisierter Polysaccharide (Dextrine) aus Starkekleister durch Microben. *Zentralbl. Bakteriol. Parasitenk. Abt. II* **1911**, *29*, 188-197.

(58) Freudenberg, K.; Jacobi, R. Uber Schardinger Dextrine aus Starke. *Liebigs Ann. Chem.* **1935**, *518*, 102-108.

(59) Freudenberg, K.; Cramer, F. Die Konstitution der Schardinger-Dextrine α, β und γ. *Z. Naturforsch* **1948**, *B3*, 464-468.

(60) Freudenberg, K.; Blomquist, G.; Ewald, L.; Soff, K. Hydrolysis and acetolysis of starch and of the Schardinger dextrins. *Berichte der Deutschen chemischen Gesellschaft zu Berlin* **1936**, *69*, 1258.

(61) Pringsheim, H. In *Chemistry of the Saccharides;* McGraw-Hill Book Company: New York, 1932; .

(62) Harada, A.; Kamachi, M. Complex formation between poly(ethylene glycol) and α-cyclodextrin. *Macromolecules* **1990**, *23*, 2821-2823.

(63) Tonelli, A. In *Molecular Processing of Polymers with Cyclodextrins;* Wenz, G., Ed.; Inclusion Polymers; Springer Berlin / Heidelberg: 2009; Vol. 222, pp 115-173.

(64) Buschmann, H. -.; Knittel, D.; Schollmeyer, E. New Textile Applications of Cyclodextrins. *Journal of Inclusion Phenomena and Macrocyclic Chemistry* **2001**, *40*, 169-172.

(65) E.M.Martin, D. V. Cyclodextrins and their uses: a review. *Process Biochemistry* **2004**, *39*, 1033-1046.

(66) Szejtli, J. Introduction and General Overview of Cyclodextrin Chemistry. *Chem. Rev.* **1998**, *98*, 1743-1754.

(67) Bullions, T.; Wei, M.; Porbeni, F.; Gerber, M.; Peet, J.; Balik, M.; White, J.; Tonelli, A. Reorganization of the structures, morphologies, and conformations of bulk polymers via coalescence from polymer-cyclodextrin inclusion compounds. *J. Polym. Sci. Pt. B-Polym. Phys.* **2002**, *40*, 992-1012.

(68) Rusa, C. C.; Rusa, M.; Peet, J.; Uyar, T.; Fox, J.; Hunt, M. A.; Wang, X.; Balik, C. M.; Tonelli, A. E. The nano-threading of polymers RID A-5886-2010. *J. Incl. Phenom. Macrocycl. Chem.* **2006**, *55*, 185-192.

(69) Shuai, X.; Probeni, F.; Wei, M.; Bullions, T.; Tonelli, A. Stereoselectivity in the formation of crystalline inclusion complexes of poly(3-hydroxybutyrate)s with cyclodextrins RID C-5819-2008. *Macromolecules* **2002**, *35*, 3778-3780.

(70) Rusa, C.; Bullions, T.; Fox, J.; Porbeni, F.; Wang, X.; Tonelli, A. Inclusion compound formation with a new columnar cyclodextrin host. *Langmuir* **2002**, *18*, 10016-10023.

(71) Tonelli, A. E. Molecular Processing of Polymers with Cyclodextrins. *Adv. Polym. Sci.* **2009**, *222*, 115-166.

(72) Wei, M.; Bullions, T.; Rusa, C.; Wang, X.; Tonelli, A. Unique morphological and thermal behaviors of reorganized poly(ethylene terephthalates). *J. Polym. Sci. Pt. B-Polym. Phys.* **2004**, *42*, 386-394.

(73) Wei, M.; Shuai, X.; Tonelli, A. Melting and crystallization behaviors of biodegradable polymers enzymatically coalesced from their cyclodextrin inclusion complexes RID C-5819-2008. *Biomacromolecules* **2003**, *4*, 783-792.

(74) Bengen, M. F. Ger. Pat. Appl. OZ 123438, 1940.

(75) Smith, A. E. The crystal structure of the urea--hydrocarbon complexes. *Acta Crystallogr.* **1952**, *5*, 224-235.

(76) Weber, E. Clathrate chemistry today — Some problems and reflections. *Top. Curr. Chem.* **1987**, *140*, 1-20.

(77) Weber, E.; Czugler, M. In *Functional group assisted clathrate formation — Scissor-like and roof-shaped host molecules;* Weber, E., Ed.; Molecular Inclusion and Molecular Recognition — Clathrates II; Springer: Berlin / Heidelberg, 1988; Vol. 149, pp 45-135.

(78) Herbstein, F. In *Structural parsimony and structural variety among inclusion complexes (with particular reference to the inclusion compounds of trimesic acid, N-(p-tolyl)-tetrachlorophthalimide, and the heilbron "complexes");* Weber, E., Ed.; Molecular Inclusion and Molecular Recognition — Clathrates I; Springer: Berlin / Heidelberg, 1987; Vol. 140, pp 107-139.

(79) Gdaniec, M. In *Channel Inclusion Compounds;* Encyclopedia of Supramolecular Chemistry; Taylor & Francis: New York, 2007; pp 223-228.

(80) Harris, K. D. M. In *Urea Inclusion Compounds;* Encyclopedia of Supramolecular Chemistry; Taylor and Francis: New York, 2007; pp 1538-1549.

(81) Vasanthan, N.; Shin, I.; Tonelli, A. Structure, conformation, and motions of poly(ethylene oxide) and poly(ethylene glycol) in their urea inclusion compounds. *Macromolecules* **1996**, *29*, 263-267.

(82) VASANTHAN, N.; SHIN, I.; TONELLI, A. Structure, Conformation, and Motions of Polytetrahydrofuran (Pthf) in the Hexagonal Form of the Pthf-Urea Inclusion Compound. *J. Polym. Sci. Pt. B-Polym. Phys.* **1995**, *33*, 1385-1393.

(83) CHOI, C.; DAVIS, D.; TONELLI, A. Inclusion Compound Formed between Poly(epsilon-Caprolactone) and Urea. *Macromolecules* **1993**, *26*, 1468-1470.

(84) HOWE, C.; VASANTHAN, N.; MACCLAMROCK, C.; SANKAR, S.; SHIN, I.; SIMONSEN, I.; TONELLI, A. Inclusion Compound Formed between Poly(l-Lactic Acid) and Urea. *Macromolecules* **1994**, *27*, 7433-7436.

(85) Chatani, Y.; Kuwata, S. Structural Investigation of Radiation-Induced Urea Canal Polymerization of 1,3-Butadiene. *Macromolecules* **1975**, *8*, 12-18.

(86) Eaton, P.; Vasanthan, N.; Shin, I.; Tonelli, A. Formation and characterization of polypropylene urea inclusion compounds. *Macromolecules* **1996**, *29*, 2531-2536.

(87) Minagawa, M.; Yamada, H.; Yamaguchi, K.; Yoshii, F. Gamma-ray irradiation canal polymerization conditions ensuring highly stereoregular (>80%) polyacrylonitrile. *Macromolecules* **1992**, *25*, 503-510.

(88) Gurarslan, A.; Tonelli, A. E. Single-Component Polymer Composites. *Macromolecules* **2011**, *44*, 3856-3861.

(89) Gurarslan, A. Single-Component Nylon-6 Composites, North Carolina State University, 2011.

(90) Haynes, W. M., Ed.; In *CRC Handbook of Chemistry and Physics, 92nd Edition;* CRC Press/Taylor and Francis: Boca Raton, FL., 2012; .

(91) WILLIAMSON, B. R. Processing Polymers with Cyclodextrins, North Carolina State University, 2010.

(92) JOIJODE, A. S. Behavior and Properties of Self-Nucleated Poly (ethylene terephthalate) (PET), North Carolina State University, 2011.

(93) Oliver, W. C.; Pharr, G. M. An improved technique for determining hardness and elastic modulus using load and displacement sensing indentation experiments. *J. Mater. Res.* **1992**, *7*, 1564-1583.

(94) Iannace, S.; De Luca, N.; Nicolais, L.; Carfagna, C.; Huang, S. J. Physical characterization of incompatible blends of polymethylmethacrylate and polycaprolactone. *J Appl Polym Sci* **1990**, *41*, 2691-2704.

(95) Doerner, M. F.; Nix, W. D. A method for interpreting the data from depth-sensing indentation instrurnents. *J. Mater. Res.* **1986**, *1*, 601-609.

(96) Oliver, W. C.; Pharr, G. M. Measurement of hardness and elastic modulus by instrumented indentation: Advances in understanding and refinements to methodology. *J. Mater. Res.* **2004**, *19*, 3-20.

(97) Vasanthan, N.; Shin, I. D.; Tonelli, A. E. Conformational and Motional Characterization of Isolated Poly(epsilon-caprolactone) Chains in Their Inclusion Compound Formed with Urea. *Macromolecules* **1994**, *27*, 6515-6519.

(98) Coleman, M. M.; Zarian, J. Fourier-transform infrared studies of polymer blends. II. Poly(ε-caprolactone)-poly(vinyl chloride) system. *Journal of Polymer Science Part B: Polymer Physics* **1979**, *17*, 837-850.

(99) Chen, E.; Wu, T. Isothermal crystallization kinetics and thermal behavior of poly(ε-caprolactone)/multi-walled carbon nanotube composites. *Polym. Degrad. Stab.* **2007**, *92*, 1009-1015.

(100) Gurarslan, A.; Shen, J.; Tonelli, A. E. Behavior of Poly(ε-caprolactone)s (PCLs) Coalesced from Their Stoichiometric Urea Inclusion Compounds and Their Use as Nucleants for Crystallizing PCL Melts: Dependence on PCL Molecular Weights. *Macromolecules* **2012**, *45*, 2835-2840.

(101) Fischer-Cripps, A. C. Critical review of analysis and interpretation of nanoindentation test data. *Surface and Coatings Technology* **2006**, *200*, 4153-4165.

(102) Bullions, T. A.; Edeki, E. M.; Porbeni, F. E.; Wei, M.; Shuai, X.; Rusa, C. C.; Tonelli, A. E. Intimate blend of poly(ethylene terephthalate) and poly(ethylene 2,6-naphthalate) via formation with and coalescence from their common inclusion compound with gamma-cyclodextrin. *Journal of Polymer Science Part B-Polymer Physics* **2003**, *41*, 139-148.

(103) Rusa, C. C.; Uyar, T.; Rusa, M.; Hunt, M. A.; Wang, X. W.; Tonelli, A. E. An intimate polycarbonate/poly(methyl methacrylate)/poly(vinyl acetate) ternary blend via

coalescence from their common inclusion compound with gamma-cyclodextrin. *Journal of Polymer Science Part B-Polymer Physics* **2004**, *42*, 4182-4194.

(104) Rusa, C. C.; Wei, M.; Shuai, X.; Bullions, T. A.; Wang, X.; Rusa, M.; Uyar, T.; Tonelli, A. E. Molecular mixing of incompatible polymers through formation of and coalescence from their common crystalline cyclodextrin inclusion compounds. *Journal of Polymer Science Part B-Polymer Physics* **2004**, *42*, 4207-4224.

(105) Tonelli, A. E. Organizational Stabilities of Bulk Neat and Well-Mixed, Blended Polymer Samples Coalesced from Their Crystalline Inclusion Compounds Formed with Cyclodextrins. *Journal of Polymer Science Part B-Polymer Physics* **2009**, *47*, 1543-1553.

(106) Uyar, T.; Aslan, E.; Tonelli, A. E.; Hacaloglu, J. Pyrolysis mass spectrometry analysis of poly(vinyl acetate), poly(methyl methacrylate) and their blend coalesced from inclusion compounds formed with gamma-cyclodextrin. *Polym. Degrad. Stab.* **2006**, *91*, 1-11.

(107) Uyar, T.; Oguz, G.; Tonelli, A. E.; Hacaloglu, J. Thermal degradation processes of poly(carbonate) and poly(methyl methacrylate) in blends coalesced either from their common inclusion compound formed with gamma-cyclodextrin or precipitated from their common solution. *Polym. Degrad. Stab.* **2006**, *91*, 2471-2481.

(108) Wei, M.; Shin, I. D.; Urban, B.; Tonelli, A. E. Partial miscibility in a nylon-6/nylon-66 blend coalesced from their common alpha-cyclodextrin inclusion complex. *Journal of Polymer Science Part B-Polymer Physics* **2004**, *42*, 1369-1378.

(109) Wei, M.; Tonelli, A. E. Compatiblization of polymers via coalescence from their common cyclodextrin inclusion compounds. *Macromolecules* **2001**, *34*, 4061-4065.